

DUST DEVILS ON EARTH AND MARS

Matt Balme^{1,2} and Ronald Greeley³

Received 12 October 2005; accepted 19 July 2006; published 23 September 2006.

[1] Dust devils, particle-loaded vertical convective vortices found on both Earth and Mars, are characterized by high rotating wind speeds, significant electrostatic fields, and reduced pressure and enhanced temperature at their centers. On Earth they are subordinate to boundary layer winds in the dust cycle and, except possibly in arid regions, are only “nuisance-level” phenomena. On Mars, though, they seem to support the persistent background atmospheric haze, to influence the surface albedo through the formation

of “tracks” on the surface, and to possibly endanger future exploration because of their high dust load and large potential gradients. High-resolution numerical simulations and thermophysical scaling models successfully describe dust devil-like vortices on Mars, but fitting dust devil action into the Martian global dust cycle is still problematic. Reliable parameterizations of their erosional abilities and solid temporal and spatial distribution data are still required to build and test a complete model of dust devil action.

Citation: Balme, M., and R. Greeley (2006), Dust devils on Earth and Mars, *Rev. Geophys.*, 44, RG3003, doi:10.1029/2005RG000188.

1. INTRODUCTION

[2] Dust devils are small whirlwinds made visible by entrained dust and sand. They are upward moving, spiraling flows caused by heating of near-surface air by insolation. The term “dust devil” is used to refer to sustained, particle-loaded convective vortices to distinguish them from vortices that form in the same way but are too weak to pick up materials and become visible. They are common atmospheric phenomena on both Earth (Figure 1) and Mars (Figure 2) and have been observed for their general characteristics, measured in situ, and simulated both numerically and in the laboratory. They are distinct from tornadoes in that they are powered only by insolation, rather than release of latent heat, and form under clear skies with no association with thunderstorms.

[3] Beginning with the descriptions of *Baddeley* [1860], there has been more than a century of dust devil investigations. Although many of these studies were performed as adjuncts to other meteorological studies, some investigations focused specifically on dust devils [e.g., *Sinclair*, 1966; *Ryan and Carroll*, 1970; *Fitzjarrald*, 1973; *Metzger*, 1999; *Renno et al.*, 2004], seeking to understand their role in convection, arid zone erosion, and sediment transport and their danger to light and unpowered aircraft. Although terrestrial dust devils have been studied in detail for decades, it is the discovery of their frequent occurrence on Mars in VO, MPF-IMP, MGS MOC NA/WA, and ODY THEMIS

and, recently, MER and MEX HRSC (see Table 1 for acronym definitions) images that motivated this general review of their properties, mode of formation, and effects on the climate of both planets.

[4] The next few decades will witness an unprecedented number of robotic missions to Mars and perhaps the first human missions. A sound understanding of the Martian environment is essential for planning such missions, and insight into dust devil processes is essential. Dust devils also affect scientific questions about climate, surface-atmosphere interaction, and the cycles of erosion and sedimentation on Mars. Now is an ideal time to crystallize the current state of knowledge on dust devils, on both Earth and Mars, and to highlight future areas of work.

2. TERRESTRIAL DUST DEVILS: GENERAL CHARACTERISTICS

2.1. Geographical and Seasonal Occurrence

[5] Dust devils usually occur in the summer in arid regions [*Ives*, 1947] such as (1) the southwest United States [*Brooks*, 1960; *Crozier*, 1964; *Sinclair*, 1964, 1965, 1966, 1969; *Carroll and Ryan*, 1970; *Crozier*, 1970; *Ryan and Carroll*, 1970; *Hallett and Hoffer*, 1971; *Ryan*, 1972; *Fitzjarrald*, 1973; *Sinclair*, 1973; *Idso*, 1974, 1975; *Schwiesow and Cupp*, 1975; *Schwiesow et al.*, 1977; *Snow and McClelland*, 1990; *Metzger*, 1999; *Balme et al.*, 2003a; *Farrell et al.*, 2003; *Houser et al.*, 2003; *Tratt et al.*, 2003; *Williams*, 1948; *Farrell et al.*, 2004; *Renno et al.*, 2004; *Towner et al.*, 2004], (2) Africa [*Durward*, 1931; *Freier*, 1960; *McGinnigle*, 1966; *Mattsson et al.*, 1993; *Rossi*, 2002], (3) Australia [*Hess and Spillane*, 1990], (4) South America [*Metzger*, 2001], and

¹Planetary Science Institute, Tucson, Arizona, USA.

²Also at Department of Earth Sciences, Open University, Milton Keynes, UK.

³Department of Geological Sciences, Arizona State University, Tempe, Arizona, USA.



Figure 1. Terrestrial dust devils. (a) Large dust devil in the distance at Eldorado Playa, Nevada, United States. The core is clearly visible with a poorly structured skirt of material near the ground. Image credit S. Metzger/M. Balme/T. Ringrose, Planetary Science Institute, Tucson, and Open University, Milton Keynes. (b) Same dust devil as in Figure 1a, ~20 m in diameter, on the playa. Note the heavy dust load. Image credit S. Metzger/M. Balme/T. Ringrose, Planetary Science Institute, Tucson, and Open University, Milton Keynes. (c) Another heavily dust-laden dust devil in Eloy, Arizona, United States. The dust devil is a few meters in diameter. The core is again clearly visible, and there is a bowl-shaped base to the dust devil. Image credit L. Neakrase, Arizona State University, Tempe. (d) A poorly defined dust devil with no clear structure. These sorts of dust devils are more common than the columnar variety but are much less photogenic. Image credit S. Metzger, Planetary Science Institute, Tucson.

elsewhere including the Middle East [Flower, 1936], China [Mattsson *et al.*, 1993], and the Canadian sub-Arctic [Grant, 1949].

[6] Sinclair [1966] suggests that convective vortices and dust devils do not form solely because of ground heating by strong insolation but as a result of vertical instability in the atmosphere wherever there is a superadiabatic atmospheric lapse rate, a source of vorticity, and a supply of sand, dust or debris. Although these conditions commonly occur in hot, arid regions during the summer, they can also occur in winter or spring when cold air spreads over warmer ground or in the cold, dry conditions of the sub-Arctic.

[7] The frequency of occurrence of dust devils is affected by many factors. The most active dust devil areas appear to be hot, flat surfaces [Mattsson *et al.*, 1993] such as dry playas and riverbeds, especially those close to freshly ploughed and irrigated fields [Sinclair, 1969]. Gentle slopes favor dust devil formation; mountains and foothills do not [Brooks, 1960]. Although they tend not to form where there is extensive tree cover [Sinclair, 1969] or grass [Metzger, 1999], the existence of vegetation per se does not preclude dust devil formation [McGinnigle, 1966; Mattsson *et al.*, 1993; Metzger, 1999]. Neither does moderate rock cover inhibit dust devil activity. For example, Metzger [1999] found that areas in Nevada with rock cover >40% contained

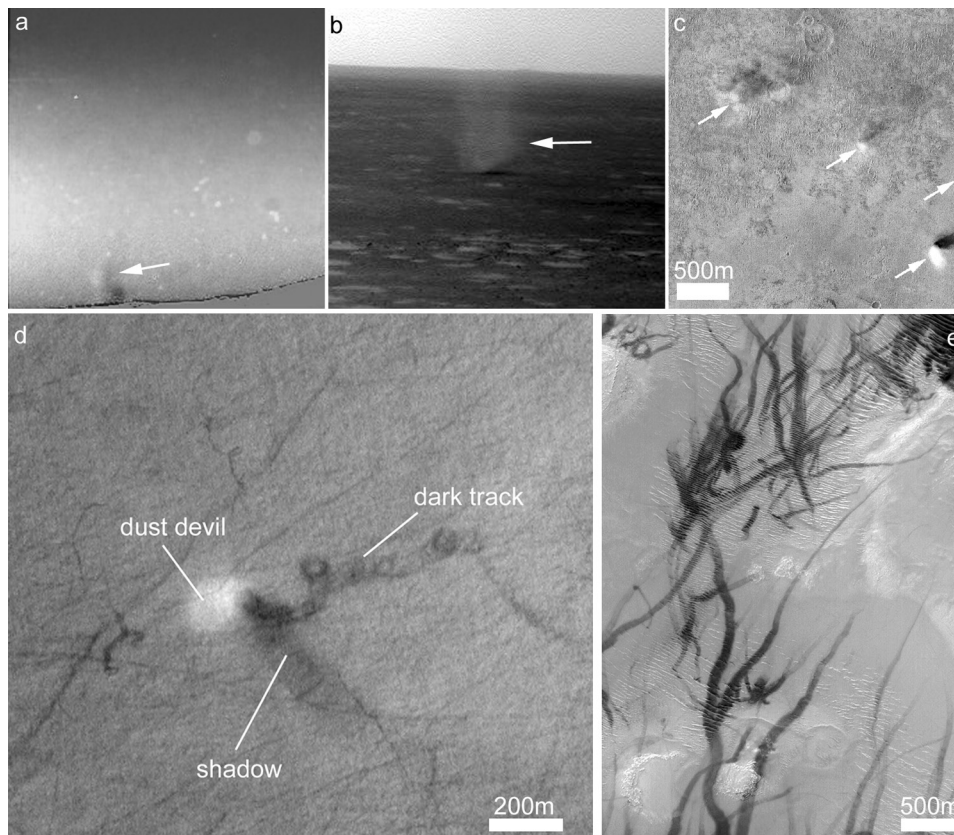


Figure 2. Dust devils on Mars. (a) False color image of a dust devil column (arrowed) observed in MPF IMP data. The dust devil was estimated to be 10–20 m in diameter [Metzger *et al.*, 1999]. Substantial image processing was required to extract the dust devil from the background haze. After Metzger *et al.* [2000]. Copyright 2000 IEEE. Figure 2a is constructed from NASA MPF images 165020033, 165020103, and 165020173. (b) Dust devil observed from the surface in a MER Spirit Navigation camera image. Note that the higher vantage point of MER compared to MPF means dust devils are much easier to see against the surface than against the dusty sky and less image processing is needed. The dust devil is at most a few tens of meters in diameter. Image number is 2N170391683ESFAAFQP1560L0M1, sol 496. Image credit NASA/Jet Propulsion Laboratory (JPL). (c) Dust devils on the surface of Mars observed from orbit. Dust devils appear as vertical dust columns (arrowed) ~100 m in diameter. Illumination is from the southwest; north is up. Figure 2c is taken from MOC NA image R1104573 (Malin Space Science Systems image of the day MOC2-600). Image credit NASA/JPL/Malin Space Science Systems. (d) An ~100 m diameter dust devil and track observed in MOC NA image M1001267. Note curlicue shape of the track. Image credit NASA/JPL/Malin Space Science Systems. (e) Multiple dust devil tracks over dune/ripple terrain. MOC NA images such as this can sometimes contain hundreds of dust devil tracks. Figure 2e is from NASA Planetary Image Atlas image PIA02376. Image credit NASA/JPL/Malin Space Science Systems.

few dust devils, but areas with rock cover of 17–25% had many observable dust devils. In the Peruvian Andes, Metzger [2001] observed boulder fields in volcanic terrain that acted as “breeding grounds” for thermal plumes and produced thousands of dust devils per week. Control of dust devil activity by topography is sometimes observed, as suggested by Williams [1948], McGinnigle [1966], Hallett and Hoffer [1971], and Hess and Spillane [1990], who report lines of dust devils forming parallel to local ridges.

[8] Ideal regional characteristics for dust devil breeding grounds are (1) frequent strong insolation, (2) arid terrain with some rock cover but few trees, buildings, or grassy areas, and (3) gently sloping topography. Sinclair [1969] suggests that ideal local conditions for dust devils include (1) a plentiful supply of loose surface material, (2) “hot

TABLE 1. Acronyms

Acronym	Definition
HRSC	High-Resolution Stereo Camera
LES	Large Eddy Simulation
MER	Mars Exploration Rover
MEX	Mars Express
MGS	Mars Global Surveyor
MOC (NA/WA)	Mars Orbiter Camera (narrow angle/wide-angle)
MPF-IMP	Mars Pathfinder–Imager for Mars Pathfinder
ODY	Mars Odyssey
THEMIS (VIS/NIR)	Thermal Emission Imaging System (visible/near infrared)
ULF	ultralow frequency
VO	Viking orbiter
VL	Viking lander

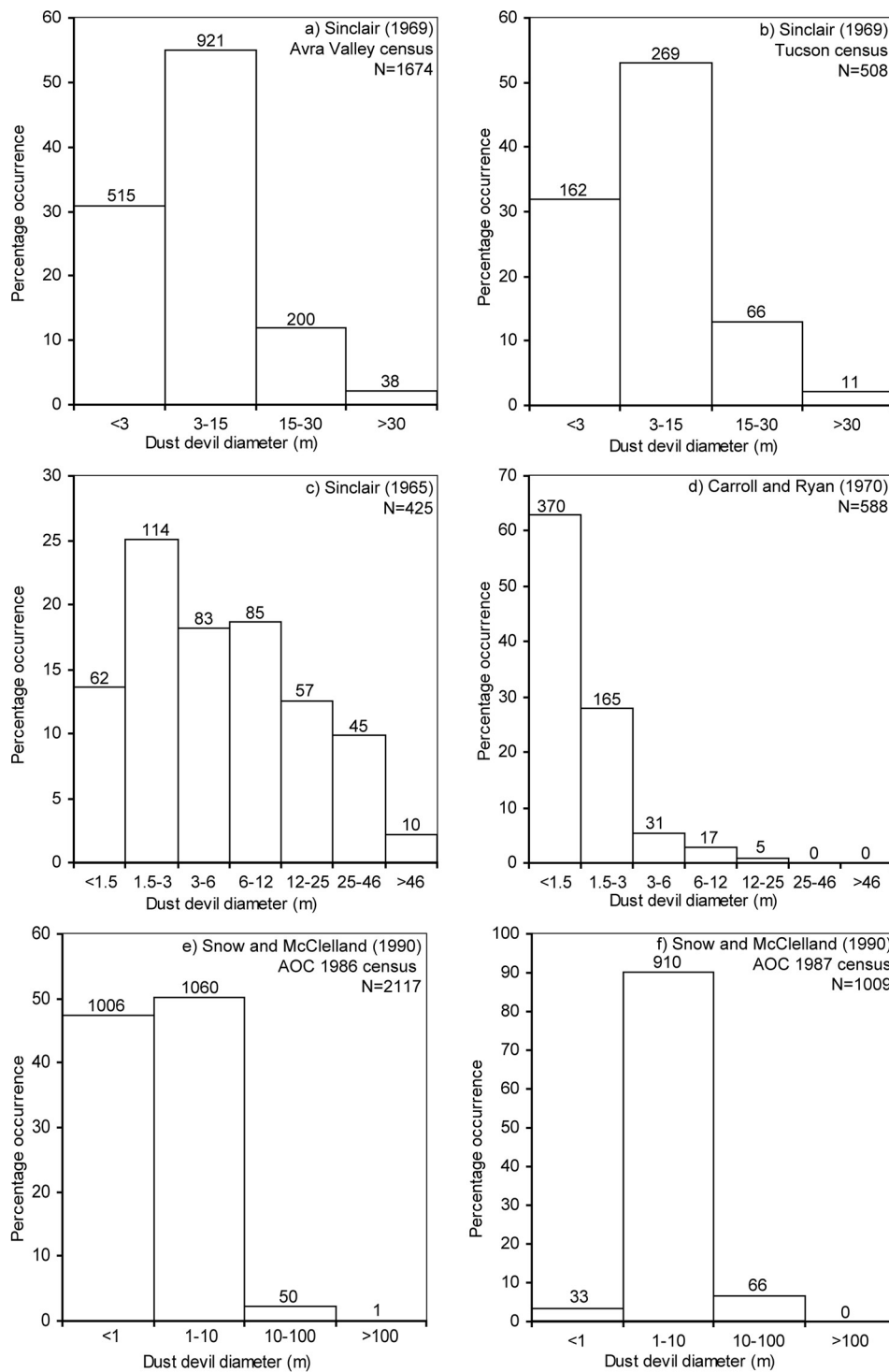


Figure 3. Dust devil diameter frequency distributions from six studies: (a) *Sinclair* [1969], Avra Valley, (b) *Sinclair* [1969], Tucson, (c) *Sinclair* [1965], (d) *Carroll and Ryan* [1970], (e) *Snow and McClelland* [1990], AOC 1985 census, and (f) *Snow and McClelland* [1990], AOC 1987 census. *N* is the total number of dust devils observed. Numbers at the top of each bar represents how many dust devils were observed in that interval. Results are from observation programs except for Figure 3c which gives combined results from *Flower* [1936], *Williams* [1948], *Sinclair's* own work, and data from the Cooperative Dust Devil Observation Program of the Institute of Atmospheric Physics, Tucson [see *Sinclair*, 1965]. Dust devil diameter of visible dust cloud at the base of the dust devils except for the results of *Snow and McClelland* [1990] shown in Figures 3e and 3f. *Snow and McClelland* [1990] categorize dust devil sizes as small, medium, large, and gigantic and use both height and diameter in classification. However, the diameter intervals shown here were their primary means of classification and were only moderated by the height to which dust was lofted.

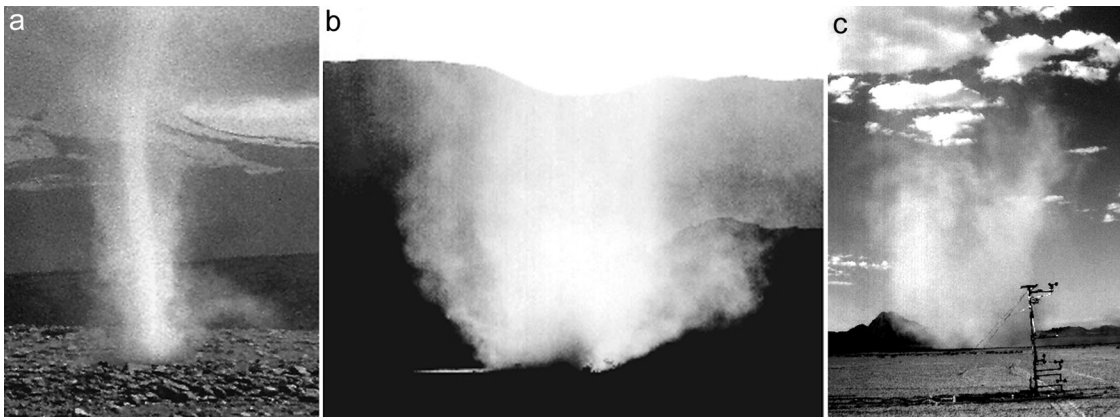


Figure 4. “Typical” dust devil morphology ranging from (a) a narrow, tightly defined column through (b) an inverted V-shaped dust cloud with a less well defined column to (c) a poorly defined inverted V shape with no visible internal column. Figure 4a is ~ 1 m in diameter; location is Sabancaya volcano, Peru. Image credit S. Metzger, Planetary Science Institute, Tucson. Figure 4b is ~ 10 m in diameter (inner column); location is Eldorado Valley, Nevada. Image credit S. Metzger, Planetary Science Institute, Tucson. Figure 4c is ~ 50 m in diameter (at ground); location is Eldorado Valley, Nevada. Dust devil monitoring equipment is visible in the foreground. Image credit S. Metzger, Planetary Science Institute, Tucson.

spots” or areas with anomalously high soil temperature, (3) local impediments to wind flow that can produce wake eddies or otherwise concentrate local vorticity, and (4) boundaries between different types of terrain (such as irrigated fields and arid desert) where strong horizontal thermal gradients can occur.

2.2. Size and Shape

[9] Most dust devils are at least 5 times higher than they are wide [Hess and Spillane, 1990], but they can be extremely tall and thin or wider than they are tall. They are most densely particle-loaded near the ground [Sinclair, 1973], and when a defined columnar core is present, it often tilts toward the direction of motion by about 10° [McGinnigle, 1966; Sinclair, 1973; Mattsson *et al.*, 1993] and can sometimes be crooked or sinuous because of wind shear.

[10] Dust devils range in height from a few meters to over 1 km and are generally less than 100 m in diameter [Mattsson *et al.*, 1993]. Data from Sinclair [1965], Flower [1936], and Williams [1948] suggest that $\sim 12\%$ of dust devils are < 3 m high, $\sim 50\%$ are 3–50 m high, $\sim 33\%$ are 50–300 m high and that only $\sim 8\%$ are > 300 m in height. Bell [1967], however, reports dust devils observed from the air that are as high as 1000–2500 m. The height of a dust devil is most likely governed by atmospheric conditions and the type of material entrained [Ives, 1947], the visible height being controlled by how much and how high the material loading the dust devil can be carried. Sinclair [1966] split the vertical structure of a “typical” dust devil into three regions. Region 1, the surface interface region, is heavily particle loaded and comprises the “vortex boundary layer” in which turbulent inflow occurs toward the center of the dust devil. Region 2, the main part of the dust devil, is characterized by a near-vertical column of rotating dust, with little exchange of dust between the column and the surrounding air [Sinclair, 1966]. Region 3, at the top of the

dust devil, is where the rotation decays and any dust is expelled into the ambient atmospheric flow.

[11] Sinclair [1965, 1969], Ryan and Carroll [1970], and Snow and McClelland [1990] made detailed statistical measurements of diameter for large samples of dust devils. The results, shown in Figure 3, have a mean diameter of ~ 7 m, with the distribution skewed toward the smaller sizes. Snow and McClelland [1990] and Metzger [1999], however, suggest that small dust devils are underreported in “spotting” surveys because of the distances from which they are observed. The exception is the study of Carroll and Ryan [1970] shown in Figure 3d that used only a 500×300 m study area. Because their study area was small, the spotting data are extremely reliable and suggest that the frequency of occurrence is inversely related to size. Renno and Bluestein [2001] suggest that available vertical atmospheric vorticity controls the diameter of dust devils, as discussed in section 5.

[12] Dust devils vary widely in morphology (Figure 4) from columnar to inverted cones to disordered, rotating dust clouds [Metzger, 1999]. Metzger [1999] found that $\sim 95\%$ of dust devils observed in the Eldorado Valley region were V-shaped, only $\sim 4\%$ being sharply defined columns. Less frequently, he observed broad rotating masses of dust with little structure but containing short-lived, dynamic “ropes.” The lower structure of a “typical” dust devil has been described as an “inverted cone with the apex touching or near the ground” [Ives, 1947; McGinnigle, 1966] or as “convex” [Sinclair, 1973] trending into a more cylindrical shape at some point above the ground (e.g., Figure 1c). In some studies [Sinclair, 1973; Balme *et al.*, 2003a], dust-free cores are present in most of the observed dust devils, but in others, dust-free cores are rare [Metzger, 1999]. Metzger [1999] suggests that different shapes of dust devils might occur in different terrain: columnar vortices being slightly more common over smooth playas and V-shaped ones

TABLE 2. Summary of Observed Sense of Rotation of Dust Devils^a

Source	N_{total}	$N_{\text{(cyclonic)}}$	$N_{\text{(anticyclonic)}}$	Notes
<i>Durward</i> [1931]	29	30	0	very small whirls, height < 1 m
<i>Flower</i> [1936]	374	199	175	
<i>Williams</i> [1948]	21	9	12	
<i>Brooks</i> [1960]	100	100	0	
<i>Sinclair</i> [1965]	144	60	84	<i>Sinclair's</i> own data
J. E. McDonald (1960)	38	9	29	reported by <i>Sinclair</i> [1965]
CDOP	88	53	35	reported by <i>Sinclair</i> [1965]
<i>Carroll and Ryan</i> [1970]	588	314	274	
<i>Fitzjarrald</i> [1973]	154	86	68	same location as <i>Carroll and Ryan</i> [1970]
Total	1536	860 (56%)	677 (44%)	

^a N_{total} is the total number of dust devils observed in the study for which rotational sense could be reliably discerned, $N_{\text{(cyclonic)}}$ is the number observed with cyclonic rotation, and $N_{\text{(anticyclonic)}}$ is the number observed with anticyclonic rotation. The totals suggest there is no preference for rotation sense. CDOP is Cooperative Dust Devil Observation Program.

found more frequently over rougher, shrubby alluvial plains. This suggests that, aside from the intensity and rotation of dust devils, the availability of different materials with different particle sizes or densities adds to the variety of morphologies observed.

[13] Finally, dust devils frequently contain subvortices [*Williams*, 1948; *Sinclair*, 1973; *Ryan and Carroll*, 1970; *Hallett and Hoffer*, 1971; *Metzger*, 1999; *Balme et al.*, 2003a] or have parasitic swirls trailing in their wake [*Williams*, 1948]. *Hallett and Hoffer* [1971] describe subvortices disappearing, splitting apart, and reforming. *Metzger* [1999] notes that individual dust devils can change in shape as they move, especially when they move into or over areas of different terrain, and sometimes virtually disappear before reforming again.

2.3. Sense of Rotation

[14] Whether dust devils have a preferred sense of rotation has been a controversial issue [*Durward*, 1931; *Flower*, 1936; *Williams*, 1948; *Sinclair*, 1965]. Table 2 summarizes measurements of rotation sense and shows that cyclonic and anticyclonic flows are equally likely, although there is a suggestion that the largest dust devils (diameter >25 m) tend toward cyclonic rotation (65% spinning cyclonically [*Sinclair*, 1965]). *Brooks* [1960] found that of 100 dust devils observed, all had cyclonic rotation but noted that it was often difficult for observers to distinguish the sense. To overcome observational problems, *Sinclair* [1965] included only close-up measurements in which two independent observers had agreed. His data show no clear preference for rotation sense, and *Brooks's* data remain anomalous. The conclusion that dust devils have no ten-

dency toward a sense of rotation agrees well with theory; estimated ratios of inertial to Coriolis effects for even the largest dust devils show that they are too small to be affected by the Earth's spin [*Morton*, 1966]. Finally, and mysteriously, there have been several observations of dust devils completely reversing their sense of rotation [*Williams*, 1948].

2.4. Diurnal Formation Rate

[15] Dust devils form most frequently in the late morning and the early afternoon [*Flower*, 1936; *Williams*, 1948; *Sinclair*, 1969; *Hallett and Hoffer*, 1971; *Snow and McClelland*, 1990; *Mattsson et al.*, 1993; *Metzger*, 1999]. Dust devils seldom form before 1000 LT or after 1730 LT [*Sinclair*, 1969; *Snow and McClelland*, 1990; *Mattsson et al.*, 1993; *Metzger*, 1999]. *Sinclair* [1969] and *Metzger* [1999] note that dust devil sizes are not constant throughout the day. *Sinclair* [1969] found that small dust devils peak in activity earlier than large ones and suggests that this reflects the time taken for a superadiabatic temperature profile to form through a deep layer of the atmosphere. However, *Metzger* [1999] reports that the tallest dust devils occurred around 1100 LT and that later in the day the height stabilizes at ~150 m.

[16] There is some evidence that dust devil formation is “bursty” and that an hour or so of intense activity is frequently followed by a more quiescent period [*Sinclair*, 1969; *Snow and McClelland*, 1990]. *Carroll and Ryan* [1970] note similar behavior but on a shorter timescale (5–15 min) and interpret the data to signify that the time-scales of atmospheric convection govern dust devil activity. *Sinclair* [1969] suggests that periods of particularly intense dust devil activity “stir up” the superadiabatic boundary

TABLE 3. Summary of Observed Dust Devil Frequency^a

Study Reference	Dates	T_s , days	N_{total}	A , km ²	Mean Activity, d ⁻¹ km ⁻²
<i>Fitzjarrald</i> [1973]	Jul–Oct	12	156	0.15	86.67
<i>Carroll and Ryan</i> [1970]	Apr–Sep	10	1151	0.15	767.33
<i>Snow and McClelland</i> [1990]	May–Aug	61	2117	64.50	0.54
<i>Snow and McClelland</i> [1990]	Apr–May	36	1017	33.80	0.84
<i>Sinclair</i> [1969], Tucson	Jun	11	610	500.00	0.11
<i>Sinclair</i> [1969], Avra Valley	Jun–Jul	22	1663	388.00	0.19

^a T_s is the length of time the study lasted, N_{total} is the total number of dust devils observed, and A is the study area size.

TABLE 4. In Situ Wind Speed Measurements in Dust Devils^a

Study Reference	N	V_{mean} , m s ⁻¹	V_{max} , m s ⁻¹	V_h mean, m s ⁻¹	V_h max, m s ⁻¹	W_{mean} , m s ⁻¹	W_{max} , m s ⁻¹
<i>Sinclair</i> [1964]	4	-	-	9.3	13	-	-
<i>Ryan and Carroll</i> [1970]	80	4.2	9.5	-	-	0.7	2
<i>Fitzjarrald</i> [1973]	11	7.3	11.5	-	-	1.3	4.25
<i>Sinclair</i> [1973]	3	10.8	11.5	-	-	13.3	15
<i>Metzger</i> [1999]	5	13.6	22	-	-	5.2	7
<i>Balme et al.</i> [2003a]	10	-	-	17.0	25	-	-
<i>Tratt et al.</i> [2003]	3	-	-	8.8	11.0	3.3	3.5

^aEach measurement represents the largest value measured from that component within each dust devil. All measurements are taken at ~ 2 m height above surface except those of *Tratt et al.* [2003], which are made at ~ 3.5 m. N is the number of dust devils sampled, V is the peak tangential component of the wind speed, V_h is the peak total horizontal wind speed, and W is the peak vertical wind speed. Subscript “mean” represents the average value for the whole study; subscript “max” represents the greatest measurement in the study.

layer to such an extent that it suppresses dust devil formation and requires some time to reestablish itself.

2.5. Lifetime and Frequency of Occurrence

[17] Terrestrial dust devils are transient events and most last for only a few minutes [*Idso*, 1974], although *Snow and McClelland* [1990] and *Metzger* [1999] observe that lifetimes might be underestimated, especially for smaller dust devils that can grow or shrink as they travel. *Metzger* [1999], *Ives* [1947], and *Mattsson et al.* [1993] report rare occurrences of large dust devils with lifetimes of 30 min to several hours. *Ives* [1947] reports a large, stationary dust devil that lasted over 4 hours and large migratory dust devils in Utah with lifetimes >7 hours that traveled ~ 60 km. *Ives* [1947], *Sinclair* [1969], and *Metzger* [1999] found that large dust devils are longer-lived than smaller ones, *Ives* [1947] suggesting an empirical relation of 1 hour of duration for every 300 m of height.

[18] The frequency of occurrence is highly dependent on the season, time of day, and location. Most studies are not representative of the wider region because, of necessity, investigations have focused on areas where dust devils form frequently. The number of dust devils observed per day depends upon the size of the study area as illustrated in Table 3, reinforcing the fact that small dust devils are often ignored. *Carroll and Ryan* [1970] found that >750 dust devils can occur per square kilometer per day.

3. SPECIFIC MEASUREMENTS OF TERRESTRIAL DUST DEVILS

[19] Detailed wind speed, pressure, temperature, and dust load measurements of dust devils can be made in situ or using remote sensing. To date, most data have been obtained in situ because current remote sensing techniques have insufficient resolution. While in situ measurements have the advantage of allowing several parameters to be sampled simultaneously, they must contend with technical challenges such as a hostile environment that can damage sensitive equipment and the short lifetimes and unpredictable nature of the phenomena; in situ measurements require robust yet mobile sampling systems [*Sinclair*, 1973; *Metzger*, 1999; *Tratt et al.*, 2003; *Metzger et al.*, 2004a]. Choice of study area is also essential; it must have frequent,

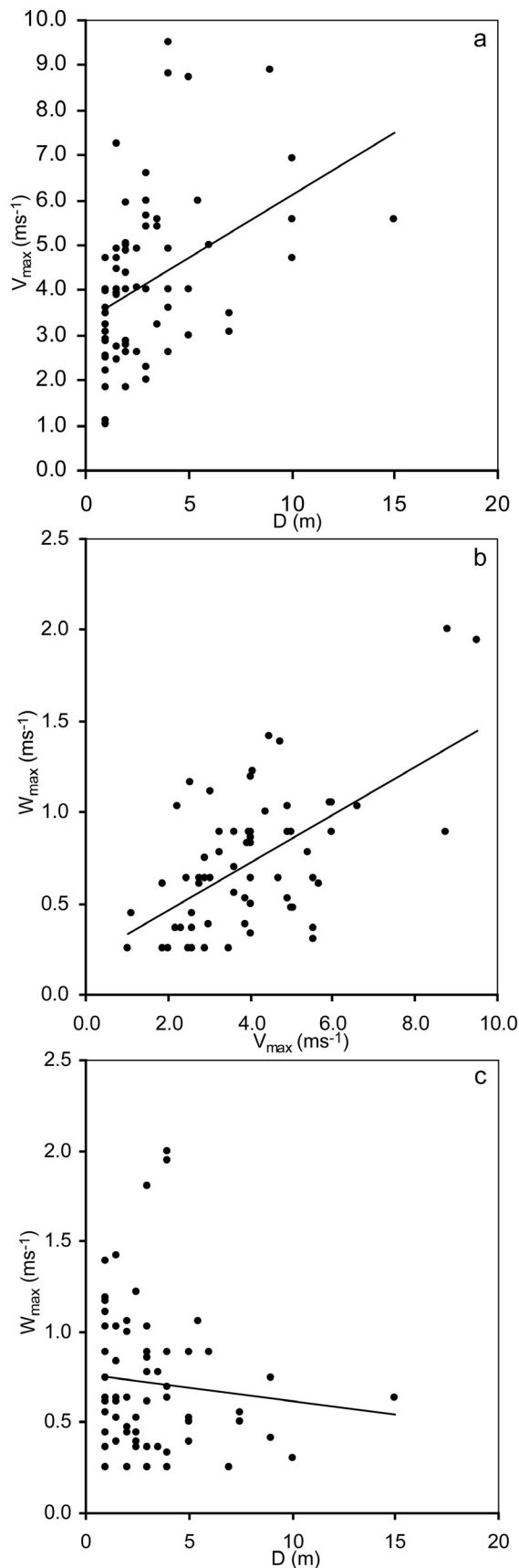
observable dust devil activity, easy vehicle access, and a surface that allows for rapid movement of the sampling system. Playas and their surrounding terrain are ideal study areas. Two playas in particular, Eldorado Valley in Nevada [*Metzger and Lancaster*, 1995; *Metzger*, 1999; *Balme et al.*, 2003a; *Metzger et al.*, 2004a, 2004b; *Towner et al.*, 2004] and another in the Mojave Desert, southern California [*Ryan and Carroll*, 1970; *Carroll and Ryan*, 1970; *Ryan*, 1972; *Fitzjarrald*, 1973], have been the site of several studies.

3.1. Wind Speed Structure of Dust Devils

[20] Wind speed measurements are either generalizations of many measurements or detailed studies of a few dust devils. Wind speeds are usually quoted as cylindrical components relative to the central point of the dust devil and include tangential velocity U , radial velocity V , and vertical velocity W . The magnitude of the total horizontal wind speed, $V_h = (V^2 + U^2)^{1/2}$, is also frequently quoted as no directional measurements are required. Commonly, for studies of multiple dust devils, only the peak values of the components are reported. Most measurements within dust devils have been made at ~ 2 m height following *Sinclair* [1964, 1973], although some measurements have been made very close to the ground [*Balme et al.*, 2003a; *Metzger et al.*, 2004b] and at heights up to ~ 23 m [*Kaimal and Bussinger*, 1970].

[21] Table 4 summarizes the “general” wind speed measurements. V is usually 5–10 m s⁻¹, with peak values up to ~ 20 m s⁻¹. V_h values up to ~ 25 m s⁻¹ have been measured in situ in approximate agreement with remote sensing measurements for V_h made using *lidar* of 11 m s⁻¹ [*Bluestein and Pazmany*, 2000] and 22 m s⁻¹ [*Schwiesow and Cupp*, 1975]. (Italicized terms are defined in the glossary, after the main text.) Vertical wind speeds are generally about a quarter of the peak rotational wind speed; only *Sinclair* [1973] and the qualitative estimates of *Ives* [1947] and *Hallett and Hoffer* [1971] suggest greater values for W . Typically, horizontal wind speeds within dust devils are <25 m s⁻¹, and vertical wind speed is <10 m s⁻¹.

[22] *Ryan and Carroll* [1970] provide a large, self-consistent data set (>80 encounters with dust devils made at the same study area with simultaneous measurements at 2 m height of V and W and estimates of diameters). Their results suggest that larger dust devils have greater rotational wind



speeds and that dust devils with greater rotational winds also tend to have greater vertical winds (Figure 5).

[23] Detailed data for the velocity structure within dust devils are limited because of the difficulties of making high-resolution in situ measurements. Horizontal profiles of wind speeds through dust devils [Sinclair, 1964, 1973; Kaimal and Bussinger, 1970; Fitzjarrald, 1973; Metzger, 1999; Balme *et al.*, 2003a; Tratt *et al.*, 2003] show that near-surface horizontal wind speed has a minimum at the center of the dust devil and a peak at a radius concurrent with the visible dust-laden region and falls to zero away from the dust devil until there is no rotation. This is particularly obvious in Figure 6 [Metzger *et al.*, 2004a], which shows wind speed measurements made in a vertical section through a dust devil. In general, the horizontal wind speed profiles approximate a Rankine vortex (Figure 7). Sinclair [1973] finds good agreement of dust devil data with the Rankine model at heights of ~ 2 m and ~ 10 m, but outside the solidly rotating central region, recent measurements [Tratt *et al.*, 2003] show that the wind speed profile is closer to an $r^{-1/2}$ distribution than r^{-1} , probably because of nonconservation of angular momentum caused by frictional losses near the surface. It is likely that the Rankine structure is applicable higher up in the dust devil where surface effects are negligible.

[24] There is almost no systematic radial flow within the dust devil core [Sinclair, 1966], radial inflow instead occurs near the ground, with radial wind speeds greatest just outside of the dust column [Sinclair, 1966, 1973]. Inflow occurs both in front of and behind the dust devil as it moves across the surface. The visible dust devil column appears to be embedded within a larger region of radial inflow. Balme *et al.* [2003a] found an approximately linear increase in horizontal wind speed with the logarithm of heights from 0.05 to 1.90 m, suggesting that the radial inflow layer was at least 2 m deep.

[25] Some researchers have found central downdrafts within dust devils [Kaimal and Bussinger, 1970; Sinclair, 1973]. Downdrafts are less intense (or not present) near the ground than at height within the dust devil devils [Kaimal and Bussinger, 1970; Sinclair, 1973]. Metzger [1999] reports that at 2 m height most dust devils have no central downdraft. This suggests a stagnation point in the vortex and reversal in the direction of vertical flow at height from zero to a few meters above the ground (Figure 8).

[26] Subvortices, ambient winds, and local gusts add to the variable nature of dust devils. However, stable, simple dust devils are characterized by (1) radial inflow near the surface (with peak inflow speeds just outside the dust column), (2) upward flow within the dust column (with

Figure 5. Wind speed data from Ryan and Carroll [1970]. (a) Peak tangential wind speed (V_{\max}) measured in each dust devil plotted against the observed dust devil diameter (D). (b) Peak vertical wind speed (W_{\max}) plotted against peak tangential wind speed. (c) Peak vertical wind speed plotted against dust devil diameter. Solid lines are linear least squares best fit lines.

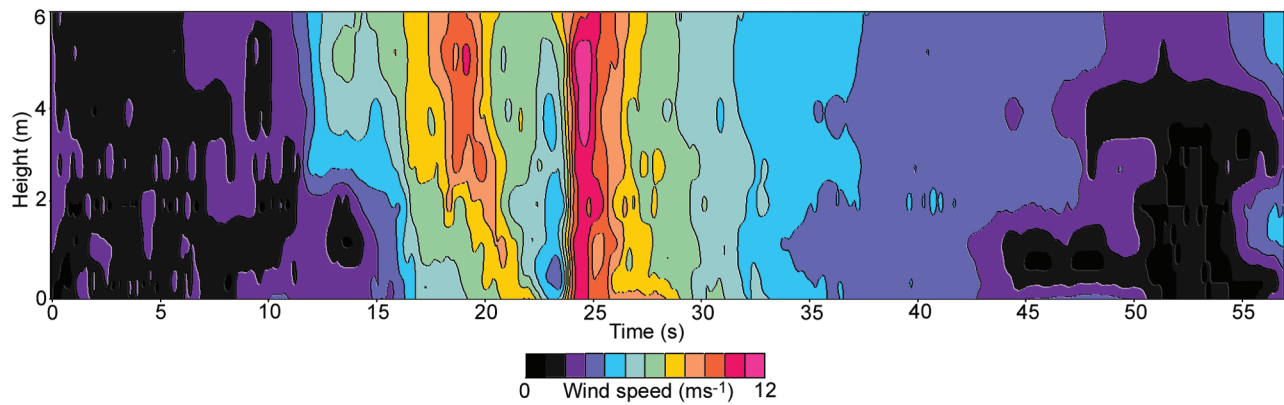


Figure 6. Time series cross section of total horizontal wind speed in a 2 m diameter dust devil from the Mojave Desert in August 2004. The dust devil is moving toward the left, and the time axis that serves as a proxy for the horizontal axis is scaled to be consistent with the height axis. Note that the peak wind speed occurs slightly outside the visible core (where there is a peak of combined radial and tangential wind speeds) and at about 4 m height in the front wall of the vortex. Note also that that high wind speeds extend almost to the ground in the back wall. After *Metzger et al.* [2004a].

possible downward flow at the center), and (3) tangential wind speeds that approximate a Rankine vortex and that peak at about the same radius as the visible dust column. At the center of the dust devil, vertical flow dominates; within the dust column, rotation and vertical flow dominate; just outside the column, inflow and rotation dominate. The most distant areas affected by the dust devils differ from the ambient winds only by weak inflow toward the dust devil. This structure is summarized in Figure 9.

[27] The higher reaches of dust devils can only be sampled remotely or from aircraft. *Sinclair* [1966] measured vertical wind speeds in “thermals” above large dust devils using an instrumented sailplane. At altitudes of 2000–4000 m, warm upwellings a few tenths of a degree above ambient with vertical wind speeds of $\sim 2\text{--}4\text{ m s}^{-1}$ covered an area of 1–5 km in diameter above large dust devils. The vertical wind speeds were often reduced at the center of the flow, and in some cases, there was weak evidence for central downdrafts. *Sinclair* [1966] also noted that surrounding these upwellings were regions of downward flow and that this structure was stable with time. This suggests that large dust devils are linked to a much larger continuous upward flow of air that extends to several kilometers height and expands to a few kilometers in diameter before returning downward. It is unknown whether this return flow can also be through the center of the thermal to link with downward flows measured near the ground at the center of some dust devils.

3.2. Temperature and Pressure Excursions Within Dust Devils

[28] Dust devil cores commonly have small, positive temperature excursions [*Sinclair*, 1964, 1973; *Fitzjarrald*, 1973; *Metzger*, 1999; *Tratt et al.*, 2003]. A summary of these measurements is given in Table 5. Temperature excursions $< \sim 10^\circ\text{C}$ are found consistently [*Sinclair*, 1969, 1973; *Tratt et al.*, 2003], but measurements with an order of magnitude higher sampling rate [*Metzger*, 1999] show temperature excursions as great as 20°C . The temperature

excursion seems to be fairly stable to heights of $\sim 3\text{ m}$ [*Tratt et al.*, 2003], but it weakens farther up in the core [*Kaimal and Bussinger*, 1970]. A cooler ring of air surrounding the warm cores has been reported [*Ives*, 1947; *Ringrose*, 2003], but available data are too poor to resolve detailed temperature structure.

[29] In addition to the positive temperature excursion, negative pressure excursions or “pressure wells” are common at the center of dust devils as first noted by *Ives* [1947] and summarized in Table 6. *Ringrose* [2003] measured pressure wells at heights of 0.04, 1.0, and 1.8 m above the ground but found no correlation between maximum pressure drop and height. Most measurements of pressure wells in dust devils are only a few millibars from

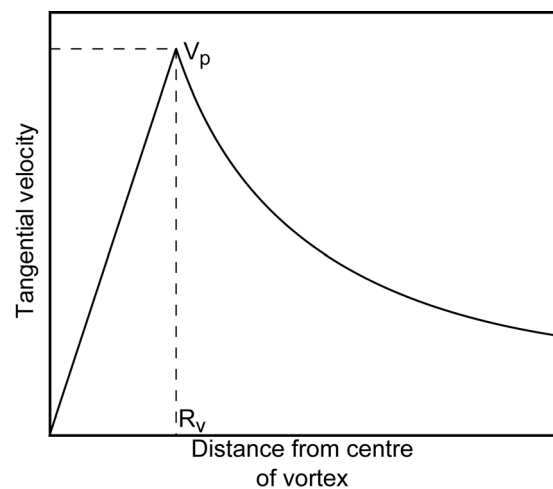


Figure 7. Rankine vortex tangential velocity structure. The vortex consists of a central region in solid rotation (tangential velocity rises as a linear function of radius) and an exterior region in potential flow (tangential velocity decreases as an inverse function of radius). Tangential velocity reaches a peak (V_p) at radius R_v at the edge of the solidly rotating region.

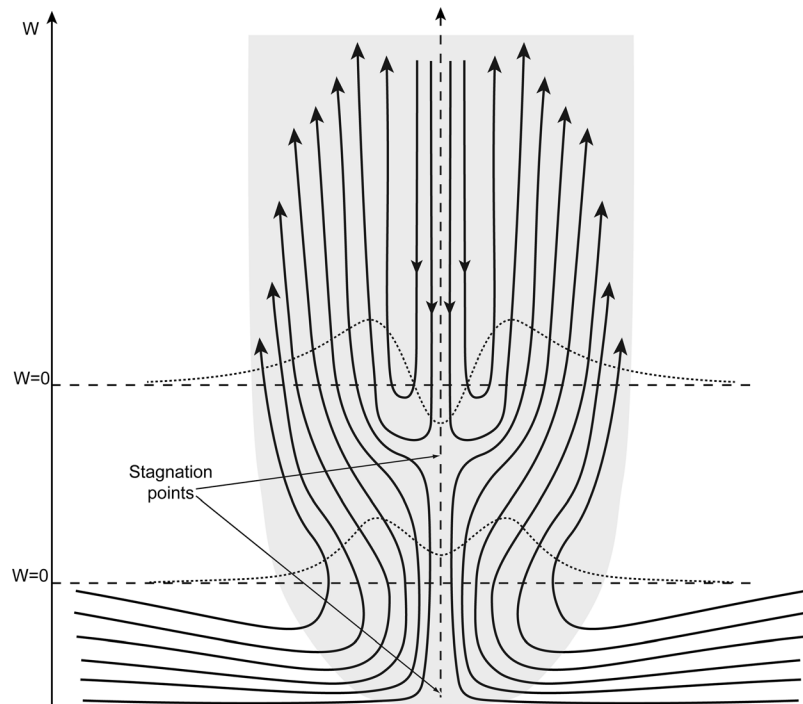


Figure 8. Sketch showing possible vertical flow in a dust devil. The solid, arrowed lines show the flow directions. The dotted lines represent the vertical wind speed profile that would be measured at that height if the dust devils' velocity field were sampled. The existence of a stagnation point above the ground level might explain why downward flow has been found at the center of dust devils at some heights above the surface but not near the ground. This might also explain why some dust devils appear to have downward flow in the core, while others do not. The reversal in flow might occur at considerable height above the surface (as shown here) or at ground level (downward flow throughout the dust devil) or might not be present at all (upward flow throughout dust devil).

ambient, but both Metzger [1999] and Ringrose [2003] measured some pressure wells about an order of magnitude larger. These might represent a small population of dust devils with exceptionally deep pressure wells (Ringrose [2003] suggests the tightest vortices have the deepest pressure wells), or they might represent a confined region of low pressure present in most dust devils but only rarely sampled, even in apparently central penetrations.

3.3. Electrical and Magnetic Structure

[30] Dust storms can generate significant electrostatic fields because of contact between grains and between grains and the surface. This process is known as the triboelectric effect and has been observed in dust devils for several decades [Freier, 1960; Crozier, 1964, 1970; Farrell *et al.*, 2003, 2004]. Table 7 summarizes the electrical measurements made in and near dust devils. Dust devils always appear to have negative electric fields, and charge densities of 10^5 – 10^7 electrons cm^{-3} are not uncommon. Farrell *et al.* [2004] suggest that the negative gradient is due to particle-size-dependent stratification caused by the tendency of small particles to become negatively charged during charging [Ette, 1971]. Thus, because the net flow in a dust devil preferentially transfers smaller particles upward compared to larger sand-grade material, a negative potential gradient is observed. Farrell *et al.* [2004] estimated the potential difference over one particular dust devil as being as large as 0.8 MV.

[31] In addition to electrostatic fields, Houser *et al.* [2003] measured AC magnetic fields around and within dust devils. They measured ultralow-frequency (3–30 Hz) emissions as a dust devil approached their instruments and noted a peak in intensity as it passed over the sensors. Interestingly, the intensity remained high for about 12 s after the dust devil had passed before decreasing to ambient levels about 30 s after the encounter. Houser *et al.* [2003] attributed this behavior to the entire dust devil radiating ULF emissions. The discovery of ULF emissions might be used in the future for remote sensing of dust devil activity or might give an indication of the “dustiness” of a vortex detected using other sensors.

3.4. Entrainment of Surface Material by Dust Devils

[32] Dust devils are erosional agents: The simple fact that they are visible means that they remove material from the surface. For example, satellite images revealed tracks over sand dunes left by the passage of dust devils [Rossi, 2002]; these dunes have bimodal particle size distributions, and it is thought that the removal of the finer sands changes the albedo compared with undisturbed areas. However, the transport of sands in dust devils occurs only locally (typical small dust devils do not travel great distances and sand is lifted within the dust devil but returns to the surface a few tens of meters from the core). However, the transport and suspension of smaller particles ($<25 \mu\text{m}$) by dust devils is

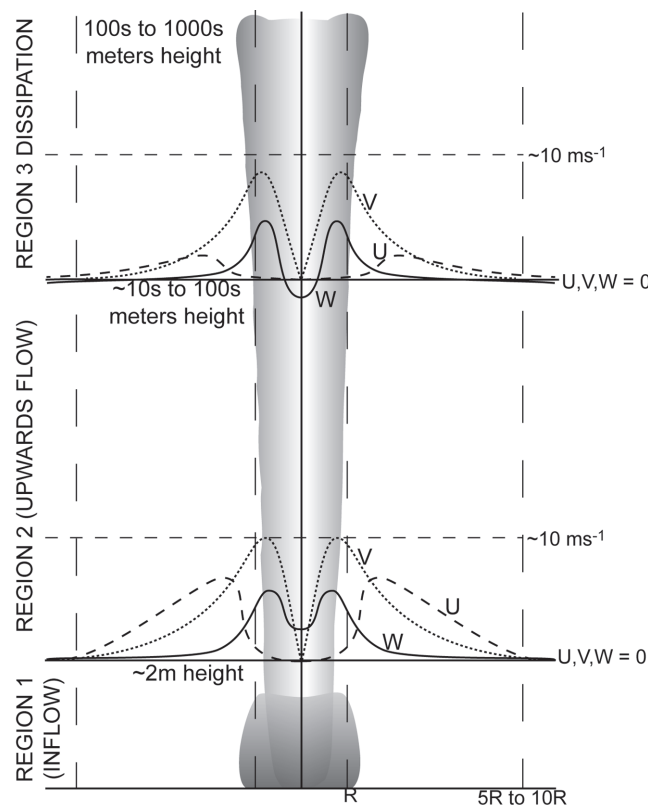


Figure 9. Generalization of wind speed within a dust devil. R is the radius of the dust column, U , V , and W are the radial, tangential, and vertical wind speeds, respectively. W is shown here to be negative at height, but it is unknown if this is representative of most or only few dust devils. Maximum speeds are given as $\sim 10 \text{ m s}^{-1}$, typical of many dust devils, but can be up to 25 m s^{-1} . Regions shown at left are after the description of *Sinclair* [1966].

important for climate, air quality, and particle transport considerations. Dust devils efficiently transport dust vertically where it can be transported in suspension by regional winds for hours or days [Gillette and Sinclair, 1990]. Mattsson *et al.* [1993] suggest that dust devils in North Africa might be a mechanism for dust injection into the atmosphere and transport into Europe.

[33] Dust flux in dust devils has been estimated by aircraft measurements of vertical velocity and particle loading in dust devils. Fluxes up to $\sim 3 \times 10^{-3} \text{ kg m}^{-2} \text{ s}^{-1}$ at heights of $\sim 140 \text{ m}$ were measured for very large dust devils [Gillette and Sinclair, 1990], but fine particles ($< 25 \mu\text{m}$) made up only about 5% of this figure ($\sim 1.6 \times 10^{-4} \text{ kg m}^{-2} \text{ s}^{-1}$). Smaller dust devils were found to lift orders of magnitude less material. Lidar measurements of dust concentrations have

TABLE 5. In Situ Temperature Excursions Measured at the Center of Dust Devils^a

Study Reference	Instrument Type	N	h , m	S , Hz	ΔT , °C
<i>Sinclair</i> [1964]	resistance thermometers	4	~ 2	~ 1	+4 to +8
<i>Sinclair</i> [1973]	resistance thermometers	3	~ 2	~ 1	+3.5 to +5
<i>Metzger</i> [1999]	sonic anemometer	~ 20	2	~ 10	+8 to +22
<i>Tratt et al.</i> [2003]	E-type thermocouples	5	1 to 3	~ 1	+1 to +3

^a N is the number of dust devils sampled, h is the height at which measurements were made, S is the effective sampling rate, and ΔT is the temperature excursion.

also been used to estimate dust fluxes; for example, *Renno et al.* [2004] estimated a particle flux of $\sim 1 \times 10^{-3} \text{ kg m}^{-2} \text{ s}^{-1}$ 100 m above the surface, and *Metzger* [1999] measured flux of $\sim 0.6 \times 10^{-3}$ to $4.4 \times 10^{-3} \text{ kg m}^{-2} \text{ s}^{-1}$ in the lower regions of dust devils. These values are similar and suggest that large, long-lived dust devils can remove hundreds or even thousands of kilograms of material from the surface during their lifetime. For the contiguous United States, *Gillette and Sinclair* [1990] estimated that dust devils might be responsible for as much as two thirds of the total

TABLE 6. In Situ Pressure-Well Measurements in Dust Devils^a

Study Reference	N	ΔP , mbar
<i>Ives</i> [1947] ^b	1	-15 to -80
<i>Sinclair</i> [1964]	4	-2.5 to -4.5
<i>Sinclair</i> [1973]	3	-2 to -7.0
<i>Metzger</i> [1999]	~ 20	0 to < -15
<i>Ringrose</i> [2003]	10	-1.5 to -10 ^c
<i>Tratt et al.</i> [2003]	5	-0.3 to -1

^a N is the number of dust devils sampled, and ΔP is the peak pressure excursion measured in each dust devil.

^bIt is likely that this measurement was misprinted in the original literature, where the value quoted was 1.5 to 2 inches of mercury. If this should have read inches of water, it would bring *Ives*' measurements more in line with modern data.

^cNine of the measurements were ~ -1.5 mbar; only one dust devil had a ΔP of -10 mbar.

TABLE 7. Electric Field Measurements of Dust Devils^a

Study Reference	<i>N</i>	<i>d</i> , m	<i>V</i> , kV m ⁻¹	CD, e ⁻ cm ⁻³	<i>D</i> , m
Freier [1960]	1	30	-0.4	NA	8
Crozier [1964]	1	450	-0.06	~1 × 10 ⁶	20
Crozier [1970]	17 (53) ^b	250	-0.04 to -1.6 (<-4) ^c	10 ⁵ -10 ⁷	10-60
Farrell et al. [2003]	1	0	<-20	NA	30
Farrell et al. [2004]		0	<-4.35	~10 ⁶	7

^a*N* is the number of dust devils sampled, *d* is the closest approach the dust devil made to the instrument, *V* is the measured electrical potential gradient, CD is the estimated charge density in the dust devils column, and *D* is the estimated dust devil diameter. NA indicates not available.

^bSeventeen measurements are presented in detail; in total, 53 measurements were made.

^cThe largest potential gradient measured was not presented in detail as it saturated the instrument at -4 kV m⁻¹.

windblown dust for particle sizes of <25 μm and that, particularly in the southwest United States and other arid regions, dust devils could be a significant cause of poor air quality. Efforts to improve regional or global models to include dust devil processes are hampered by the fact that they fall below the resolution of most models. *Cakmur et al.* [2004] initiated studies to parameterize dust lifting by local circulation into global climate models, but much remains to be done.

[34] To complement field studies of dust devils, laboratory simulations and experiments are also conducted under controlled conditions. Vortex simulators have been used to model the dynamics of tornadoes and dust devils for several decades and have mainly focused on initiation and dynamics of the flows, but there have been some studies focused on particle lifting as well. Work using a vortex generator [*Hsu and Fattahi*, 1976] reported by *Greeley et al.* [1981] and *Greeley and Iversen* [1985] suggested that the horizontal shear stresses caused by swirling winds might be assisted in lifting particles by a “vacuum cleaner” effect caused by the low-pressure core associated with dust devil vortices. Later, using an apparatus specifically designed to simulate the particle-lifting action of terrestrial and Martian dust devils, *Greeley et al.* [2003] confirmed that for dust size particles, dust devil vortices are more efficient at entraining material than their wind speeds alone account for. They suggest that the pressure well effect (referred to as the Δ*P* effect) is the probable cause. *Neakrase et al.* [2004] have used the same apparatus to estimate the rates that these laboratory vortices remove dust from the surface and find excellent agreement with the field data reported above (0.2 × 10⁻³ to 5 × 10⁻³ kg m⁻² s⁻¹ in the laboratory compared with *Metzger’s* [1999] field measurements of 0.6 × 10⁻³ to 4.4 × 10⁻³ kg m⁻² s⁻¹). This work is ongoing but reinforces fieldwork results that dust devils can play a dominant role in transporting dust into the atmosphere and reducing air quality in arid regions.

4. DUST DEVILS ON MARS

4.1. Background

[35] Dust devils were first identified on Mars in VO images as small bright clouds with long tapered shadows [*Thomas and Gierasch*, 1985], although their existence had been hypothesized previously [*Neubauer*, 1966; *Gierasch*

and *Goody*, 1973]. Many dozens of dust devils were found in VO images, but when high-resolution MOC images became available, many more dust devils on Mars were identified [*Edgett and Malin*, 2000; *Malin and Edgett*, 2001] (Figures 2c and 2d). Dust devils have also been observed in MEX HRSC images [*Stanzel et al.*, 2005]. In addition to active dust devils, “tornado tracks” [*Grant and Schultz*, 1987], later shown to be dust devil tracks [*Edgett and Malin*, 2000], are seen in huge numbers in MOC NA images. Dust devils were also imaged directly from the surface by MPF IMP [*Metzger et al.*, 1999] (Figure 2a) and the MER Spirit (Figure 2b), and meteorological data were used to infer their passage over the Viking [*Ryan and Lucich*, 1983; *Ringrose et al.*, 2003] and MPF [*Schofield et al.*, 1997; *Murphy and Nelli*, 2002] landers. Because of the difficulty of obtaining in situ data, techniques such as laboratory and numerical simulations have also been extensively employed to understand particle-lifting and formation mechanisms of Martian dust devils.

4.2. General Appearance and Size

[36] Mars orbiter observations of active dust devils show that they are frequently a few kilometers high and hundreds of meters in diameter and tend to have narrow bases and broader tops [*Thomas and Gierasch*, 1985]. Up to 10 dust devils have been observed in a single MOC WA frame [*Edgett and Malin*, 2000; *Malin and Edgett*, 2001]. Table 8 shows that Martian dust devils can be an order of magnitude larger than terrestrial ones but that there are also many smaller examples that can probably only be detected from the surface. Recent images from MER (e.g., NASA MER Spirit press release, 19 August 2005, <http://marsrovers.jpl.nasa.gov/gallery/press/spirit/20050819a.html>) have confirmed earlier observations from IMP [*Metzger et al.*, 1999, 2000] that Martian and terrestrial dust devils are similar in morphology (compare Figure 2b and Figures 1a–1c) and can be extremely common.

[37] Dust devil tracks have been used to estimate dust devil diameter. *Edgett and Malin* [2000], *Malin and Edgett* [2001], and *Balme et al.* [2003b] note that most dust devil tracks are a few to tens of meters wide and that the diameters of the dust devils that formed them are presumably similar. The largest tracks observed are up to a few hundreds of meters in diameter, in agreement with images of active dust devils.

TABLE 8. Summary of Observation of Martian Dust Devils^a

Study Reference	Data Source	<i>N</i>	<i>H</i> , km	<i>D</i> , m
<i>Direct Imaging Methods^b</i>				
<i>Thomas and Gierasch</i> [1985]	Viking (orbiter)	~100	1 to 2.5	70 to 1000
<i>Wennmacher et al.</i> [1996]	Viking (orbiter)	~30	mean ~1.3	~100
<i>Edgett and Malin</i> [2000]	MOC WA (orbiter)	NA	≤6	NA
<i>Metzger et al.</i> [1999]	MPF IMP (lander)	5	0.05 to 0.25	15 to 80
<i>Biener et al.</i> [2002]	MOC WA (orbiter)	NA	0.4 to 2.6	<1750
<i>Ferri et al.</i> [2003]	MPF IMP (lander)	14	NA	15 to 550
<i>Fisher et al.</i> [2005]	MOC NA (orbiter)	≥20	0.17 to 1.8	28 to 509
<i>Fisher et al.</i> [2005]	MOC WA (orbiter)	≥14	3.8 to 8.5	NA
<i>Indirect Methods^c</i>				
<i>Ferri et al.</i> [2003]	MPF ASI/MET	19	NA	mean ~200 ^d
<i>Ryan and Lucich</i> [1983]	Viking 1 Lander Met	40	NA	10 to 700
<i>Ryan and Lucich</i> [1983]	Viking 2 Lander Met	78	NA	10 to 950
<i>Ringrose et al.</i> [2003]	Viking 2 Lander Met	8	NA	20 to 450 ^e

^a*N* is the number of dust devils observed, *H* is the height of the dust devil, and *D* is the diameter. Definitions are ASI, atmospheric structure investigation; MET, meteorology experiment; and Viking Met, Viking lander meteorology experiment.

^bDirect observations of the dust column are obtained by orbiting or surface-based cameras.

^cSizes are estimated from excursions in meteorological data.

^dAn ambient wind speed of 10 m s⁻¹ is assumed.

^eOnly “core sampling” or “near miss” events are included (type 1 and 2 given by *Ringrose et al.* [2003]).

4.3. Seasonal Dependence, Diurnal Activity, and Geographic Distribution

[38] The long lifetimes of the Viking landers and orbiters and MGS missions allow multiyear observation and measurement of active dust devils from orbit and in situ. These studies show that dust devil activity follows the season of maximum insolation [*Ryan and Lucich*, 1983; *Thomas and Gierasch*, 1985; *Cantor and Edgett*, 2002]. Most dust devil tracks are seen in images taken during regional spring and summer [*Balme et al.*, 2003b]; these observations also show that the tracks “fade” on a timescale much shorter than one Martian year.

[39] Analysis of ~80 convective vortices recorded by MPF [*Murphy and Nelli*, 2002] shows a clear trend in diurnal activity: Most vortices occur between 1200 and 1300 local time, as seen for terrestrial dust devils. Analysis of Viking Lander 2 data by *Ringrose et al.* [2003] shows a less clear pattern, although the peak is still 1200 LT. Moreover, these data show “bursts” of dust devil formation with fewer events in the half hour after a period of intense activity as seen on Earth.

[40] Determining where dust devils form most frequently on Mars is challenging because of the sheer volume of data. Over 100,000 MOC images of suitable resolution have been taken, and still more are being acquired. With only a very small percentage containing active dust devils, searching the whole set is an enormous task, although progress is being made to automate the process [*Gibbons et al.*, 2005]. Surveys of dust devil tracks have been made as a proxy for active dust devils, but data volume still limits these to only regional studies [e.g., *Balme et al.*, 2003b; *Fisher et al.*, 2005]. Some particularly active dust devil regions that have been identified include northern hemisphere low-lying regions such as Amazonis Planitia (~30°N, ~190°E [*Edgett and Malin*, 2000; *Fisher et al.*, 2005; *Cantor and Edgett*, 2002]), Casius (~40°N, ~90°E [*Fisher et al.*, 2005]), and

the large impact basin in the southern hemisphere, Argyre Planitia (~50°S, ~340°E [*Balme et al.*, 2003b]). *Fisher et al.* [2005] observed many active dust devils in Amazonis but relatively few dust devil tracks and many dust devil tracks but no active dust devils in Casius, perhaps suggesting that dust devil tracks are not a good proxy for dust devil activity. *Geissler* [2005] found many more dust devil tracks between 45° and 60°N in the dark terrain of Nilosyrtis (~45°N, ~85°E) than in either bright or dark terrain to the south and a similar increase in the number of dust devil tracks between 40° and 60°S in Phaethontis (~50°S, ~210°E). *Grant and Schultz* [1987] and *Balme et al.* [2003b] also found dust devil tracks to be most abundant between 50° and 60°S.

[41] *Balme et al.* [2003b] suggest that dust abundance on the surface (using albedo as a proxy) might control the formation of dust devil tracks; where there is more dust, more tracks will occur. However, taking all the regional studies performed to date together, there is no clear correlation with albedo [e.g., *Geissler*, 2005], and a more global, latitudinal control seems more likely. While these data are not exhaustive, they suggest enhanced dust devil erosion at latitudes of between 30° and 65° in both hemispheres but also that dust devil activity is regionally highly variable.

4.4. In situ Measurements of Wind Speed, Sense of Rotation, Pressure, and Temperature

[42] Excursions in meteorological data made by the Viking 1 and 2 and MPF landers remain the only in situ measurements of active Martian dust devils; the recent MERs did not carry any dedicated meteorology instruments. There is a paucity of wind speed data in particular because of calibration problems with the MPF wind sensor [*Schofield et al.*, 1997]. Also, it is generally unknown whether each detection represents a convective vortex or a particle-laden dust devil because it is difficult to infer if the

vortex is dust-loaded (although one encounter with MPF was associated with a drop in power to the solar cells and was thus assumed to be a dust-loaded vortex [Schofield *et al.*, 1997]). Maximum wind speeds of up to 42 m s^{-1} at 1.6 m height were calculated for convective vortices passing over the Viking 1 and 2 landers from meteorology data by *Ryan and Lucich* [1983]. They estimated that wind speeds of $>30 \text{ m s}^{-1}$ were required to entrain surface material and therefore that seven of the detected vortices were dust devils. Peculiarly, most of the highest wind speed measurements were made during winter. Reexamining these data, *Ringrose et al.* [2003] found seven events in which a vortex had passed over the Viking 2 lander and developed an algorithm to search wind speed and direction data excursions for “near misses” by vortices. Wind speeds of up to 46 m s^{-1} at 1.6 m height were calculated for vortices that passed directly over the instruments, but wind speeds of up to $\sim 100 \text{ m s}^{-1}$ were inferred (using the Rankine vortex approximation as described in section 3.1) for vortices that passed within about five core radii of the sensors. *Ringrose et al.* [2003] used a friction wind speed threshold criterion to determine whether the vortices were dust-laden and found that only a few inferred “near-miss” examples were sufficiently vigorous to entrain material.

[43] Rotation sense was inferred using patterns of wind direction data. Neither *Ryan and Lucich* [1983] nor *Ringrose et al.* [2003] found any preference for rotation sense despite the fact that the larger size of Martian dust devils suggests they would be more influenced by planetary rotation than terrestrial ones.

[44] In contrast to the wind speed instrumentation the MPF pressure sensors were more suited to detecting vortices than the Viking instruments, which had too slow a sample rate for detection of vortices [*Ryan and Lucich*, 1983]. *Murphy and Nelli* [2002] identified 79 possible convective vortices from MPF pressure data and recorded pressure drops from ~ 0.5 to $\sim 5 \text{ Pa}$ (~ 0.075 to $\sim 0.75\%$). Over half of these encounters had pressure drops less than 1 Pa with relatively few “large” or intense (possibly dust loaded) vortices.

[45] Positive temperature excursions within vortices measured by the Viking and MPF landers had maximum values of 5–6 K. These values are similar to terrestrial measurements. However, most of the measurements had low sample rates, and it is possible that higher sampling rates would give higher peak temperature excursions, as has been the case for Earth.

4.5. Entrainment of Surface Material by Dust Devils on Mars

[46] As on Earth, observations of active dust devils and tracks indicate that they entrain surface material. Albedo decreases of at least 15% have been recorded for regions where dust devil tracks cover $\sim 50\%$ of the surface [*Geissler*, 2005]. Another indicator that dust devils inject significant material into the atmosphere locally is the close match of diurnal variations in dust opacity observed by MPF [*Smith*

and *Lemmon*, 1999] with the times when dust devil activity is greatest (midday through midafternoon).

[47] It is difficult to make quantitative estimates of how much material Martian dust devils can entrain as there have been no in situ measurements of dust/sand loading. It is also unknown whether devils tracks indicate complete removal of a dust layer or represent “jostling” and infiltration of dust into a sandy surface [*Greeley et al.*, 2005], making estimates from observations of tracks difficult. Nevertheless, optical depth measurements of dust columns were made from orbit and surface observations and used to estimate their particle load. *Thomas and Gierasch* [1985] estimated optical depths of 0.3–0.5 along the path of illumination for dust devils in Viking orbiter images and calculated the dust loading to be $3 \times 10^{-5} \text{ kg m}^{-3}$, assuming that the particles were $10 \mu\text{m}$ and the occluded path length was 250 m. Using a similar technique for MPF IMP images, *Metzger et al.* [1999] found that dust devil columns were ~ 3 – 4% darker than the sky. They estimate that the dust load was $\sim 10^{-5}$ to $10^{-4} \text{ kg m}^{-3}$, similar to the results of *Thomas and Gierasch* [1985].

[48] Extrapolating these measurements of dust load to a reliable estimate of flux is complicated by several uncertainties: (1) Estimates of vertical wind velocity within Martian dust devils can only be based on terrestrial analogues ($\sim 7 \text{ m s}^{-1}$ [*Metzger et al.*, 1999]) or first-order modeling ($\sim 20 \text{ m s}^{-1}$ [*Renno et al.*, 2000; *Ferri et al.*, 2003; *Renno et al.*, 2004]). (2) It is unknown if the entire observed dust column is moving upward or if a downwelling central core is sometimes present as for Earth. (3) It is unknown how much material removed from the surface is expelled from the top of the dust devil and how much is “recycled” within the column and immediately redeposited. (4) It is unknown what area beneath the dust column is actively entraining material. Therefore, while these data can be used to indicate dust removal flux for single Martian dust devils, a conservative estimate of the uncertainty on the measurements is approximately 2–3 orders of magnitude.

[49] Even larger uncertainties exist when trying to estimate flux from measurements of dust devil tracks. To convert observations of area and frequency of formation of tracks to a removal flux requires in situ measurements of how much material is removed per track coupled with measurement of the length of time it took to be emplaced. These data are unavailable for dust devils on both Earth and Mars. Recent MER Spirit Microscopic Imager observations have shown that sand particles within a dark linear feature (possibly a dust devil track) appear to have been cleaned of fine dust particles compared with the surface outside of the dark linear feature [*Greeley et al.*, 2005]. *Metzger* [2005] estimates that $\sim 50\%$ of the dust cover was removed from a rock by a dust devil at the MER Gusev site but acknowledges the difficulty of estimating the total mass of material actually removed by the dust devil and in what time period.

[50] Laboratory modeling of dust lifting using a vortex generator apparatus has been extended to Martian surface pressures [*Greeley et al.*, 2003]. Similar to the simulations of terrestrial atmospheric conditions, *Greeley et al.* [2003]

TABLE 9. Rossby Numbers for Dust Devils on Earth and Mars^a

Dust Devil Type	V , m s ⁻¹	2Ω	L , m	Ro
Earth (typical)	10	10^{-4}	10	2×10^3
Earth (extreme)	20	10^{-4}	100	5×10^2
Mars (typical)	30 ^b	10^{-4}	100 ^c	4×10^2
Mars (extreme)	100 ^d	10^{-4}	2000 ^e	1×10^2

^a V is peak tangential wind speed in the dust devil, Ω is the angular velocity of rotation of the planet, L is the length scale of the flow (in this case the diameter of the dust devil), and Ro is Rossby number. Higher wind speeds have been attributed to larger dust devils [Metzger, 1999].

^bValue is from Ryan and Lucich [1983].

^cValue is from Ferri et al. [2003].

^dValue is from Ringrose et al. [2003].

^eValue is from Biener et al. [2002].

found that the particle-lifting ability of vortices does not diminish as rapidly for grain sizes $>100 \mu\text{m}$ as it does for boundary layer winds, implying that vortices are the more efficient mechanism for lifting dust. Further experiments using this apparatus at Martian pressures seek to measure dust removal flux by laboratory vortices. Preliminary results suggest suspension loads of $\sim 1 \times 10^{-4} \text{ kg m}^{-3}$ are obtainable for vortices with ΔP values of 0.7% of ambient pressure (L. D. V. Neakrase, personal communication, 2005), similar to estimates from observations made on Mars.

5. DUST DEVIL FORMATION

5.1. Overview

[51] Dust devils form when surface insolation leads to a *superadiabatic lapse rate*, causing an unstably stratified atmosphere and strong convection. Dust devils appear to get their energy only from this insolation in contrast to tornadoes, which are powered in part by the release of latent heat within the column. In particular, the strength of the superadiabatic lapse rate in the region ~ 0.3 to 10 m above the surface seems to control the frequency and size of dust devils formed [Ryan and Carroll, 1970; Carroll and Ryan, 1970], stronger superadiabatic lapse rates being associated with more and larger dust devils. “Burstiness” in formation rates [Sinclair, 1969; Carroll and Ryan, 1970; Snow and McClelland, 1990] suggests that intense convection temporarily inhibits dust devil formation because of overmixing of the adiabatic layer. Dust devils do not appear to be isolated convective phenomena and instead form a part of the local convective system [Sinclair, 1966; Kaimal and Bussinger, 1970; Ryan and Carroll, 1970; Hess et al., 1988]. Observations of thermal plumes several kilometers above large dust devils [Sinclair, 1966] suggest that a dust devil is the near-surface expression of a convective plume that has been somehow “spun-up,” larger examples probably extending over the depth of the whole convective boundary layer. However, it is unclear what governs the size, wind speed, pressure, and temperature excursions and frequency of formation of dust devils and why these particular convective elements form concentrated vortices when others form thermal plumes with little or no rotation.

[52] Recent advances in numerical simulations of atmospheric dynamics, both for the Earth and Mars, have allowed investigation of convective phenomena at previously unprecedented spatial and temporal resolution. Mesoscale LES atmospheric models for Earth [Kanak et al., 2000; Kanak, 2005] and Mars [Rafkin et al., 2001; Michaels and Rafkin, 2001; Toigo and Richardson, 2002; Toigo et al., 2003] have begun to utilize resolutions sufficiently fine that they spontaneously generate convective vortices on similar scales to dust devils (although these models cannot deduce if the vortex would be dust loaded or not). The model vortices agree well with field measurements, showing similar pressure wells and diurnal behavior and velocity structure similar to real life dust devils. Models have the advantage that all vortex properties are instantly accessible, and it is likely that future work on dust devil initiation will rely heavily on such numerical simulations.

5.2. Vorticity Source

[53] While terrain features are undoubtedly responsible for the rotation of some dust devils [Sinclair, 1969; Hallett and Hoffer, 1971], many form in flat regions with weak ambient winds [Mattsson et al., 1993], and thus another source of vorticity is required. Such sources might include concentration of vorticity from planetary rotation, mesoscale eddies, or kilometer-scale swirls or tipping of horizontal vorticity (i.e., horizontal boundary layer vortices) into the vertical plane. Because dust devils do not appear to show a preference for rotational direction, it is unlikely that the planetary rotation is the source of vorticity for dust devils as shown by considerations of Rossby number, Ro, the ratio of inertial and Coriolis forces for a flow system [Morton, 1966] given by

$$\text{Ro} = V/2\Omega L, \quad (1)$$

where V is a flow speed, L is a length characteristic of the flow, and Ω is the vertical component of the angular velocity of the planet’s rotation. Table 9 shows estimated values of Rossby number for terrestrial and Martian dust devils. Even for very large dust devils the Rossby numbers are orders of magnitude >1 , implying that Coriolis forces are insignificant and that vorticity does not come directly from planetary rotation.

[54] In a field study correlating local vorticity with observations of frequency of dust devil formation and sense of rotation, *Carroll and Ryan* [1970] and *Fitzjarrald* [1973] found that the horizontal scale of vorticity variations were of the order of hundreds of meters. *Carroll and Ryan* [1970] also found that groups of dust devils with the same sense of rotation occurred often and that for larger ambient wind speeds, sense of dust devil rotation and measured vorticity were frequently in agreement. Dust devils were noted to form in areas with no local topographic obstacles or observed mesoscale phenomena [*Carroll and Ryan*, 1970], indicating that dust devils form from local sources of vorticity that change sign and amplitude with temporal scales of minutes and spatial scales of hundreds of meters. Observations that dust devils frequently occur near the boundary of irrigated fields [*Sinclair*, 1969] led *Renno et al.* [2004] to suggest that horizontal atmospheric vortices formed from opposition of cold and warm air currents that were then twisted into the vertical by convection might be a vorticity source for dust devils. Similarly, the importance of convective tipping of horizontal vorticity in dust devil formation is demonstrated in extremely high resolution numerical LES simulations [*Kanak et al.*, 2000; *Kanak*, 2005] that show vortices forming within convergent branches of convective cells. These models simulate environments with no mean winds, wind shears, or topography; vortices of similar scale and structure to dust devils are generated purely through the action of convection. Dust devil-like vortices were observed in LES models of the Martian atmosphere [*Rafkin et al.*, 2001; *Toigo et al.*, 2003], and tilting of horizontal vorticity into the vertical plane by convection appears to be the preferred formation mechanism for Martian dust devils [*Toigo et al.*, 2003].

[55] Although there is likely a variety of vorticity sources for dust devils, these results show that those that form in flat terrain with little mean wind are unlikely to be caused by large-scale (mesoscale atmospheric circulation or planetary rotation) or small-scale (spin-off from obstacles) vorticity sources. Instead, medium-scale tilting of horizontal vorticity by convection is the more probable mechanism.

5.3. Thermodynamics and Energy Balance of Dust Devils

[56] The thermophysical “Renno” model [*Renno et al.*, 1998; *Renno and Bluestein*, 2001; *Renno et al.*, 2004] describes a dust devil as a heat engine. Steady state vortices in *cyclostrophic* balance are modeled assuming that heat input is from sensible heat flux at the surface, that heat output is from thermal radiation of air parcels subsiding outside of the vortex, and that losses are due to mechanical friction at the surface. Thus the intensity of the vortex can be described by its thermodynamic efficiency (the fraction of the heat input converted into work (η) and the fraction of the total mechanical energy consumed by friction near the ground (γ)) and the thermal properties of the atmosphere. For the complete derivation readers should refer to *Renno et al.* [1998], but the important points are summarized here as this model has been applied to both Earth and Mars. *Renno*

et al. [2004] state that the bulk pressure drop across a convective circulation is

$$\Delta p \equiv (p_\infty - p_0) \approx p_\infty \left\{ 1 - \exp \left[\left(\frac{\gamma\eta}{\gamma\eta - 1} \right) \left(\frac{c_p}{R} \right) \left(\frac{\Delta T}{T_\infty} \right) \right] \right\}, \quad (2)$$

where p_0 is the surface pressure at the center of the convective circulation, T_∞ and P_∞ are the temperature and pressure away from the influence of the circulation, R is the appropriate gas constant for the atmosphere, c_p is the specific heat capacity at constant pressure for the atmosphere, and ΔT is the temperature perturbation for convective plumes over homogeneous surfaces given by *Renno and Ingersoll* [1996] as

$$\Delta T \approx \left(\frac{c_p \eta F_{\text{in}}}{8\epsilon\sigma_R g H T_c^2} \right), \quad (3)$$

where F_{in} is the surface heat flux, ϵ is the atmosphere’s emissivity, σ_R is the Stephan-Boltzmann constant, g is the acceleration due to gravity, H is the depth of the convective layer, and T_c is the temperature at the tropopause (the height at which the upward traveling warm air is assumed to be ejected from the convective system).

[57] Thus, from (2), if $\eta \ll 1$ and $\Delta p/p_\infty \ll 1$ (as would be expected for a typical convective plume or vortex), then the pressure drop can be approximated by

$$\Delta p \approx \frac{\gamma\eta c_p p_\infty \Delta T}{R T_\infty}, \quad (4)$$

and so, if the vortex is in cyclostrophic balance,

$$V_{\text{max}} \approx \left(\frac{\gamma\eta c_p \Delta T}{p_\infty} \right)^{1/2}, \quad (5)$$

where V_{max} is the peak tangential wind speed.

[58] Thus the wind speed and peak pressure excursion of a dust devil depend only upon the thermodynamics of its heat engine, which is governed by ambient conditions. Vortex size, according to *Renno and Bluestein* [2001], is proportional to the background vorticity and must be accounted for separately.

[59] This model is powerful in that it is simple, applicable to almost all environments, and describes a scaling relationship between key measurable parameters for individual dust devils. Also, measurable ambient parameters can be used to predict some properties of local dust devils from equations (3), (4), and (5). Predictions from (5) agree well with preliminary measurements of actual dust devils [*Tratt et al.*, 2003], but a statistically valid number of reliable in situ measurements has not been made, nor have detailed ambient measurements been made temporally and spatially close enough to sampled dust devils to test the validity of (3). Nevertheless, this model has been successfully extended to Mars: *Renno et al.* [2000] show that this model generates realistic temperature excursions and wind speeds when applied to measurements of pressure excursions by MPF, and *Toigo et al.* [2003] show that pressure excursions

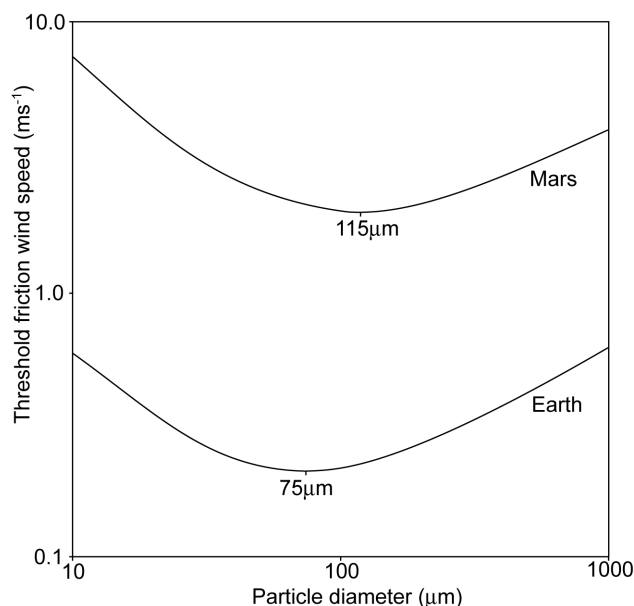


Figure 10. Boundary layer threshold friction wind speed curves for silicate density material for terrestrial and Martian conditions. Friction wind speed is defined as the square root of the ratio of the shear stress to the fluid density. Note that for both Earth and Mars the most easily lifted particle sizes are in the range for very fine sand (~ 75 or $\sim 115 \mu\text{m}$ diameter) and that for finer material the surface friction wind speed required to initiate movement is much higher. After *Greeley and Iversen* [1985].

predicted by this model agree well with numerical models (although they note that even better agreement is obtained using a lower estimate of mixing depth of 5–6 km rather than ~ 45 km as used by *Renno et al.* [2000]).

[60] A recent observation by *Lorenz and Myers* [2005] using thermal imaging suggests that material within the dust devil column is strongly heated by insolation and likely warms the air that supports it. If this is the case, then insolation of the lowest, most particle-laden parts of dust devils provides an important, and hitherto poorly recognized, contribution to the energy budget of the system. Also, this mechanism could serve as a positive feedback system (the more intense the dust devil, the dustier it becomes, therefore absorbing more solar energy and becoming even more intense) that might explain the long lifetimes of particularly large and dusty dust devils.

6. EFFECTS OF DUST DEVILS ON THE MARTIAN CLIMATE

[61] The Martian atmosphere is thinner than Earth's with a surface pressure of ~ 5.2 mbar [*Young*, 1971] compared to ~ 1000 mbar for Earth, so much higher wind speeds are required to pick up sand or dust on Mars. Wind tunnel studies [*Greeley et al.*, 1976, 1981; *Iversen and White*, 1982] have shown that, like Earth, particles with diameter 80–100 μm (fine sand) are the easiest to move, having the

lowest static threshold friction velocity, and that larger and smaller particles require stronger winds to entrain them into the flow (Figure 10). However, much of Mars' atmospheric dust load is very small ($\leq 2 \mu\text{m}$ [*Pollack et al.*, 1979, 1995; *Smith and Mars Pathfinder Team*, 1997; *Tomasko et al.*, 1999; *Lemmon et al.*, 2004]), and the boundary layer wind speeds required to entrain such fine material are in excess of those measured on the surface [*Hess et al.*, 1977; *Schofield et al.*, 1997; *Magalhaes et al.*, 1999] or predicted by climate models [*Haberle et al.*, 1999]. Nevertheless, fine dust is somehow being injected into the atmosphere to support the observed haze and to supply local [*Cantor et al.*, 2001] and global (reviewed by *Kahn et al.* [1992] and *Zurek et al.* [1992]) dust storms. *Greeley et al.* [1992] reviewed alternatives to direct lifting by boundary layer winds to raise dust, of which saltation impact (of easily moved sand into more difficult to move dust) has, until recently, been the prime candidate and has been used as the dust-lifting scheme in GCMs [*Newman et al.*, 2002].

[62] Given that dust devils were observed to be efficient transporters of fine material on Earth, they were proposed as a dust-lifting mechanism and possible triggers for global dust storms on Mars [*Neubauer*, 1966; *Gierasch and Goody*, 1973] even before they were identified in Viking orbiter images by *Thomas and Gierasch* [1985]. However, the increase in the number of observations of dust devils from MGS has led to renewed interest in dust devils and how they might affect the Martian climate. Also, recent observations of the high interannual repeatability of Martian atmospheric temperatures [*Clancy et al.*, 2000; *Richardson*, 1998; *Liu et al.*, 2003; *Smith*, 2004] seem to preclude slow fallout of dust from global dust storms as the source of the haze [*Basu et al.*, 2004], suggesting that dust devils or small convective dust storms might instead play a role in maintaining the background dustiness.

[63] Approximately $2 \times 10^{-2} \text{ kg m}^{-2} \text{ yr}^{-1}$ of dust must be removed from the Martian surface to support the observed atmospheric haze [*Pollack et al.*, 1979], a value confirmed by dust settling rates found at the MPF landing site [*Rover Team*, 1997], and so the following question is posed: Can dust devils account for this amount of dust lifting? *Balme et al.* [2003b] using dust devil track densities observed in Argyre Planitia and Hellas Basin as an estimate for the mean of the whole of the Martian surface found that dust devils alone could not account for this flux but stressed that it is unknown what percentage of dust devils leave tracks, an observation supported by a lack of consistency between areas of high dust devil track density and areas observed to have frequent active dust devils [*Fisher et al.*, 2005]. *Ferri et al.* [2003] estimate that the local dust devil removal flux from the MPF site was an order of magnitude larger than required to support the background haze, and *Fisher et al.* [2005] estimate that the dust devils flux in Amazonis was an order of magnitude higher still.

[64] The differences in these studies highlight the problem of making global estimates from limited or local data sets, and it seems that an estimate of the total dust flux can only be made from orbiter observations of tracks or active

dust devils. The two approaches can be summarized by equation (6) for active dust devils and equation (7) for dust devil tracks. For observations of active dust devils,

$$D \approx N\bar{F}\bar{L}\bar{A}, \quad (6)$$

where D is the total dust devil dust removal per year, N is the global number of dust devils that occur per Martian year, \bar{F} is the mean removal flux for dust devils on Mars, \bar{L} is the mean lifetime for a dust devil on Mars, and \bar{A} is the mean instantaneous area each dust devil acts upon. The main advantages of this scheme are that it uses observations of active dust devils and that the number of dust devils observed in images from orbiters can be calibrated by lander images from the same sites. Another advantage is that it might be possible to estimate F by combining the Renno model with results from threshold and flux experiments and data on the availability of surface dust at a given site. Disadvantages of this method include the poor resolution and limited temporal and spatial coverage of images, possibly leading to poor statistics, and a failure to include the smaller, and perhaps most common, dust devils. Also, it is difficult to estimate flux per dust devil from simulations or from lander observations without dedicated sampling systems on Mars. For observations of dust devil tracks,

$$D \approx \frac{1}{\alpha} [N_t \bar{A}_t \bar{m}_t], \quad (7)$$

where α is the fraction of all dust devils that leave tracks, N_t is the number of tracks formed on Mars per year, \bar{A}_t is the area of the average dust devil track, and \bar{m}_t is the mean mass of material removed per unit area to form a track. The biggest challenges this technique faces are estimating how much removed material a typical track represents and estimating α for given locations and seasons. Again, lander observations are likely to be vital here (recent observations have provided some preliminary data [Metzger, 2005]), but laboratory simulations of the effects of vortices on analogue surfaces will also be important.

[65] It is likely that empirical measurements will not prove sufficiently accurate to answer the question, and another technique must be employed. Recently, schemes to model dust devil flux within GCMs were developed [Newman *et al.*, 2002; Basu *et al.*, 2004]. In these schemes, dust flux by dust devil lifting is calculated at scales below the resolution of the climate model as a function of atmospheric parameters determined in the GCM. Alongside the dust devil parameterization is a boundary layer scheme that relies on saltation impact to trigger dust lifting.

[66] Both Newman *et al.* [2002] and Basu *et al.* [2004] used the Renno thermodynamic model to derive a value of dust devil activity, Λ , based only on the sensible surface heat flux (from insolation), the depth of the boundary layer, and a tunable “efficiency parameter.” Newman *et al.* [2002] used two parameterizations, one in which the dust devil injection flux was simply proportional to Λ and another that used a threshold criterion from early laboratory dust devil threshold experiments [Greeley and Iversen, 1985]. Basu *et*

al. [2004] did not use a specific dust-devil-lifting threshold criterion. Newman *et al.* [2002] tuned their scheme to match observations of opacity and presented their results in arbitrary units of flux, whereas Basu *et al.* [2004] tuned their free parameter to match year-round air temperature and used the “best fit” value to determine Λ .

[67] Newman *et al.* [2002] found that dust devil activity was greatest in a broad band at $\sim\pm 30^\circ$ latitude in each hemisphere’s summer and that a dustier atmosphere led to less dust devil activity. Very little lifting occurred poleward of 40° latitude in either hemisphere. Both Newman *et al.* [2002] and Basu *et al.* [2004] found Amazonis to be an area of particularly high dust devil erosion in agreement with observations. Basu *et al.* [2004] also found peak activity at middle/low latitudes in summer. In addition, the average northern hemisphere dust flux required to verify that their model corresponds well with the measurements of dust devil flux from MPF [Ferri *et al.*, 2003]. Basu *et al.* [2004] note that their dust devil scheme alone cannot initiate dust storms but that their boundary layer scheme cannot initiate dust storms and at the same time maintain the haze. Recent observations of active dust devils and tracks [Cantor and Edgett, 2002; Balme *et al.*, 2003b] also show no evidence for dust devils triggering dust storms. The modeling tends to confirm observations that dust devils are not triggers for global dust storms but probably are responsible for maintaining the haze.

[68] The latitudinal distributions of dust devil activity found in both models do not agree with the observed distribution of dust devil tracks discussed in section 4.3. Whether this is due to a lack of observational data or a flaw in the models is unknown. However, neither model accounts for the actual availability of dust at the surface, and factoring in this parameter perhaps from the dust cover index of Ruff and Christensen [2002] might enhance the agreement. The combination of observations and modeling suggests that dust devils are the dominant process for maintaining the Martian haze, although confirmation awaits a global study of active dust devils or tracks.

7. ARE DUST DEVILS HAZARDS TO THE EXPLORATION OF MARS?

[69] On Earth, dust devils do not form significant hazards to humanity. There are isolated reports of dust devils damaging temporary or half-built buildings [Idso, 1974], weather stations, and outdoor storage yards [Ives, 1947], and certainly, they can be a hazard to light aircraft during takeoff or landing [Hess and Spillane, 1990], but, in general, their main threat is to air quality in arid regions [Gillette and Sinclair, 1990; Mattsson *et al.*, 1993].

[70] On Mars, dust devils are often very large but are unlikely to pose a great physical threat. Although their wind speeds are poorly constrained, they are likely $\sim 100 \text{ m s}^{-1}$, and while such speeds would be devastating on Earth, the thin Martian atmosphere means they likely will be no more harmful than dust devils on Earth. Close observations of MER images of dust devils might be searched for evidence

of larger clods or pebbles in the flow as this might indicate stronger winds than exist on Earth and could suggest dust devils being more dangerous. The high particle content in dust devils was thought to pose a degradation hazard to solar panels on landing craft, but MER results have shown that the passage of a dust devil or wind gust over the lander actually cleared air-deposited dust from the solar panels, thus improving their output. However, the high particle density in dust devils might pose another risk: electrical damage through triboelectric charging. *Farrell et al.* [2004] have shown that terrestrial dust devils can have huge potential gradients, and if the same is true on Mars, this could be a significant source of electrical hazard to landers. Even though no reports of damage caused by passage of dust devils over either MPF or MER have been made, making detailed measurements is still worthwhile. Another statistic that mitigates against dust devils as a hazard is that locally they are relatively uncommon; *Ferri et al.* [2003] estimate that the instantaneous fractional area coverage of dust devil activity is only $\sim 2 \times 10^{-4}$. However, as some MOC images show regions with many orders of magnitude more dust devils than this, dust devil activity must be taken into account when selecting sites for future exploration.

8. CONCLUSIONS AND FUTURE WORK

[71] Dust devils are widespread and common phenomena on Earth, occurring throughout the world especially in arid areas. They are efficient erosional agents and can lift substantial amounts of dust-grade particles even when the ambient wind speeds are below the predicted threshold velocity for a given region. Few attempts have been made to quantify the effect of dust devils on climate, although preliminary results have shown that dust devils could form a significant part of the dust transport cycle.

[72] On Mars, dust devils are also widespread and common, and more effort has been made to integrate their effects into the global dust cycle than on Earth because of the absence of competing mechanisms to replenish the background dust haze. Recent modeling agrees with many of the observations from orbit and the surface and suggests that dust devils are the main mechanism for day-to-day dust injection. Dust devils are also responsible for local and regional changes in surface albedo, which might have a longer-term effect on climate through changing the rate of surface heating. There is no evidence that dust devils are responsible for triggering global dust storms. Their potential as hazards to robotic and human exploration has not yet been fully assessed. A key conclusion from this work is that terrestrial and Martian dust devils are alike in many ways. They have similar morphologies and similar pressure and temperature excursions (relative to the ambient atmospheric conditions). Numerical and laboratory modeling shows that dust devils on both planets form part of the larger convective system and have similar strong erosional effects on the surface.

[73] The Renno thermodynamic model has been used to describe individual dust devils on Earth and Mars and as a basis for dust devil dust-lifting schemes in GCMs. The model suggests that the intensity of a dust devil is a function of the surface heat flux from insolation and the depth of the planetary boundary layer. One of the primary tasks of future dust devil fieldwork on Earth must be to test this theory with thorough observations of ambient meteorological conditions together with detailed measurements of pressure and velocity within mature dust devils, specifically testing equations (3), (4), and (5). Other important terrestrial investigations include (1) fieldwork to obtain horizontal profiles of flux within the dust column at some height above the “sand skirt” to estimate the dust transport properties of dust devils; (2) more measurements of surface shear stress and entrained particle sizes within the lowest levels of dust devils to better constrain the dynamics of particle lifting within dust devils; (3) further laboratory tests of flux and threshold at scales as appropriate to reality as possible to support measurements outlined in item 2; and (4) fieldwork in Niger (the only known terrestrial example of dust devil tracks) to determine how dust devil tracks are formed and what amount of material is removed to create visible tracks.

[74] Future work on dust devils on Mars includes (1) a global study to measure the distribution of dust devils to obtain data from observations of active dust devils and supported by observations of dust devil tracks that will be essential for validating GCM models and important in hazard assessment for a given location; (2) more in situ measurements on Mars to determine electrical and dust hazard potential and provide “calibration” of numbers, sizes, and diurnal formation rates for orbiter images of the same region; and (3) measurements of wind speeds, pressure wells, and temperatures both of ambient conditions and within dust devils to test the Renno model and to constrain the particle-lifting abilities of dust devils on Mars. Because of the difficulties involved with making in situ measurements, developing remote sensing techniques and instruments that can be deployed on Mars is a priority.

[75] Finally, it is likely that only high-resolution numerical models will allow a full understanding of dust devil formation, and as such they must be integrated into GCM models. Bridging the gap in resolution between local LES models and GCM models is not likely to be accomplished in the near term simply by using faster computers; some degree of parameterization of activity is needed. Similarly, empirical laboratory results for flux and threshold for particle lifting by vortices seem to be the only available option for developing a reliable dust-lifting scheme, and they must also be integrated into numerical models. A modern GCM that includes parameterization of dust devil formation and dust-lifting ability, together with good remote sensing and in situ data on the type and availability of surface materials, will provide a powerful tool in understanding the global climate and surface interactions of dust devils on Mars and on Earth.

GLOSSARY

Rankine vortex: A simple two-dimensional model of swirling flow in which the tangential velocity increases linearly with radius until a characteristic radius, at which point the tangential velocity then decreases as the inverse of radius. This means that vorticity is constant within the characteristic radius and zero outside it.

Superadiabatic lapse rate: A lapse rate (vertical change in temperature) steeper than the dry adiabat (the lapse rate at which a dry parcel of air rising in the atmosphere cools without exchanging energy to the surroundings). Superadiabatic lapse rates usually only occur near the surface as a result of insolation of dry soil under clear skies and windless conditions.

Cyclostrophic: In a swirling flow a case in which the pressure gradient and centripetal forces are balanced.

Lidar: Specifically Doppler lidar. Used to remotely determine the velocity of particles in a dust devil. A laser beam is directed at the dust devil, and the wavelength change of light reflected from the entrained dust is measured. This allows precise measurements of the wind speed, but the temporal resolution can be poor.

[76] **ACKNOWLEDGMENTS.** The authors wish to thank Steve Metzger, Martin Towner, and Lynn Neakrase for constructive discussions.

[77] The Editor responsible for this paper was Gerald North. He thanks two anonymous technical reviewers and one anonymous cross-disciplinary reviewer.

REFERENCES

- Baddeley, P. F. H. (1860), *Whirlwinds and Dust Storms of India*, Bell and Daldey, London.
- Balme, M., S. Metzger, M. Towner, T. Ringrose, R. Greeley, and J. Iversen (2003a), Friction wind speeds in dust devils: A field study, *Geophys. Res. Lett.*, *30*(16), 1830, doi:10.1029/2003GL017493.
- Balme, M. R., P. L. Whelley, and R. Greeley (2003b), Mars: Dust devil track survey in Argyre Planitia and Hellas Basin, *J. Geophys. Res.*, *108*(E8), 5086, doi:10.1029/2003JE002096.
- Basu, S., M. I. Richardson, and R. J. Wilson (2004), Simulation of the Martian dust cycle with the GDFL Mars GCM, *J. Geophys. Res.*, *109*, E11006, doi:10.1029/2004JE002243.
- Bell, F. (1967), Dust devils and aviation, report, *Meteorol. Note 27*, Aust. Bur. of Meteorol., Melbourne, Victoria.
- Biener, K. K., P. E. Geissler, A. S. McEwen, and C. Leovy (2002), Observations of dust devils in MOC wide angle camera images, *Lunar Planet. Sci.* [CD-ROM], *XXXIII*, Abstract 1048.
- Bluestein, H. B., and A. L. Pazmany (2000), Observations of tornadoes and other convective phenomena with a mobile, 3-mm wavelength, Doppler radar: The spring 1999 field experiment, *Bull. Am. Meteorol. Soc.*, *81*, 2939–2951.
- Brooks, H. B. (1960), Rotation of dust devils, *J. Meteorol.*, *17*, 84–86.
- Cakmur, R. V., R. S. Miller, and O. Torres (2004), Incorporating the effect of small-scale circulations upon dust emission in an atmospheric general circulation model, *J. Geophys. Res.*, *109*, D07201, doi:10.1029/2003JD004067.
- Cantor, B. A., and K. S. Edgett (2002), Martian dust devils: 2 Mars years of MGS MOC observations, *Eos Trans. AGU*, *83*(47), Fall Meet. Suppl., Abstract P41A.
- Cantor, B. A., P. B. James, M. Caplinger, and M. J. Wolff (2001), Martian dust storms: 1999 Mars Orbiter Camera observations, *J. Geophys. Res.*, *106*, 23,653–23,689.
- Carroll, J. J., and J. A. Ryan (1970), Atmospheric vorticity and dust devil rotation, *J. Geophys. Res.*, *75*, 5179–5184.
- Clancy, R. T., M. J. Sandor, M. J. Wolff, P. R. Christensen, M. D. Smith, J. C. Pearl, B. J. Conrath, and R. J. Wilson (2000), An intercomparison of ground-based millimeter, MGS TES and Viking atmospheric temperature measurements: Seasonal and inter-annual variability of temperature and dust loading in the global Mars atmosphere, *J. Geophys. Res.*, *105*, 9553–9572.
- Crozier, W. D. (1964), The electric field of a New Mexico dust devil, *J. Geophys. Res.*, *69*, 5427–5429.
- Crozier, W. D. (1970), Dust devil properties, *J. Geophys. Res.*, *75*, 4583–4585.
- Durward, J. (1931), Rotation of ‘dust devils’, *Nature*, *128*(3227), 412–413.
- Edgett, K. S., and M. C. Malin (2000), Martian dust raising and surface albedo controls: Thin, dark (and sometimes bright) streaks and dust devils in MGS high-resolution images, *Lunar Planet. Sci.* [CD-ROM], *XXXI*, Abstract 1073.
- Ette, A. I. I. (1971), The effect of Hermatidian dust on atmosphere electrical parameters, *J. Atmos. Terr. Phys.*, *33*, 295–300.
- Farrell, W. M., G. T. Delory, S. A. Cummer, and J. Marshall (2003), A simple electrodynamic model of a dust devil, *Geophys. Res. Lett.*, *30*(20), 2050, doi:10.1029/2003GL017606.
- Farrell, W. M., et al. (2004), Electric and magnetic signatures of dust devils from the 2000–2001 MATADOR desert tests, *J. Geophys. Res.*, *109*, E03004, doi:10.1029/2003JE002088.
- Ferri, F., P. H. Smith, M. T. Lemmon, and N. O. Rennó (2003), Dust devils as observed by Mars Pathfinder, *J. Geophys. Res.*, *108*(E12), 5133, doi:10.1029/2000JE001421.
- Fisher, J. A., M. I. Richardson, C. E. Newman, M. A. Szwarcst, C. Graf, S. Basu, S. P. Ewald, A. D. Toigo, and R. J. Wilson (2005), A survey of Martian dust devil activity using Mars Global Surveyor Mars Orbiter Camera images, *J. Geophys. Res.*, *110*, E03004, doi:10.1029/2003JE002165.
- Fitzjarrald, D. E. (1973), A field investigation of dust devils, *J. Appl. Meteorol.*, *12*, 808–813.
- Flower, W. D. (1936), Sand devils, *London Meteorol. Off. Prof. Notes*, *5*(71), 1–16.
- Freier, G. D. (1960), The electric field of a large dust devil, *J. Geophys. Res.*, *65*, 3504.
- Geissler P. (2005), Three decades of Martian surface changes, *J. Geophys. Res.*, *110*, E02001, doi:10.1029/2004JE002345.
- Gibbons, A., F. Yang, P. Mlsna, and P. Geissler (2005), Automated procedures for detecting Martian dust devils, *Lunar Planet. Sci.* [CD-ROM], *XXXVI*, Abstract 2005.
- Gierasch, P., and R. M. Goody (1973), A model of a Martian great dust storm, *J. Atmos. Sci.*, *30*, 749–762.
- Gillette, D. A., and P. C. Sinclair (1990), Estimation of suspension of alkaline material by dust devils in the United-States, *Atmos. Environ. Part A*, *24*(5), 1135–1142.
- Grant, C. G. (1949), Dust devils in the sub-arctic, *Weather*, *4*, 402–403.
- Grant, J. A., and P. A. Schultz (1987), Possible tornado-like tracks on Mars, *Science*, *237*, 883–885.
- Greeley, R., and J. Iversen (1985), *Wind as a Geologic Process on Earth, Mars, Venus and Titan*, Cambridge Univ. Press, New York.
- Greeley, R., R. N. Leach, B. R. White, J. Iversen, and J. B. Pollack (1976), Mars: Wind friction speeds for particle movement, *Geophys. Res. Lett.*, *3*, 417–420.
- Greeley, R., B. White, J. B. Pollack, J. Iversen, and R. N. Leach (1981), Dust storms on Mars: Considerations and simulations, in *Desert Dust: Origin, Characteristics, and Effect on Man*, edited by T. Pêwé, *Spec. Pap. Geol. Soc. Am.*, *186*, 101–121.
- Greeley, R., N. Lancaster, S. Lee, and P. Thomas (1992), Martian Aeolian processes, sediments and features, in *Mars*, edited by H. H. Kieffer et al., pp. 730–766, Univ. of Ariz. Press, Tucson.
- Greeley, R., M. R. Balme, J. D. Iversen, S. Metzger, B. Mickelson, J. Phoreman, and B. White (2003), Martian dust devils: Labora-

- tory simulations of particle threshold, *J. Geophys. Res.*, 108(E5), 5041, doi:10.1029/2002JE001987.
- Greeley, R., et al. (2005), Martian variable features: New insights from the Mars Express Orbiter and the Mars Exploration Rover Spirit, *J. Geophys. Res.*, 110, E06002, doi:10.1029/2005JE002403.
- Haberle, R. M., M. M. Joshi, J. R. Murphy, J. R. Barnes, J. T. Schofield, G. Wilson, M. Lopez-Valverde, J. L. Hollingsworth, A. F. C. Bridger, and J. Schaeffer (1999), General circulation model simulations of the Mars Pathfinder atmospheric structure investigation/meteorology data, *J. Geophys. Res.*, 104, 8957–8974.
- Hallett, J., and T. Hoffer (1971), Dust devil systems, *Weather*, 26, 247–250.
- Hess, G. D., and K. T. Spillane (1990), Characteristics of dust devils in Australia, *J. Appl. Meteorol.*, 29, 498–507.
- Hess, G. D., K. T. Spillane, and R. S. Lourenz (1988), Atmospheric vortices in shallow convection, *J. Appl. Meteorol.*, 27, 305–317.
- Hess, S. L., R. M. Henry, C. B. Leovy, J. A. Ryan, and J. E. Tillman (1977), Meteorological measurements from the surface of Mars: Viking 1 and 2, *J. Geophys. Res.*, 82, 4559–4574.
- Houser, J. G., W. M. Farrell, and S. Metzger (2003), ULF and ELF magnetic activity from a terrestrial dust devil, *Geophys. Res. Lett.*, 30(1), 1027, doi:10.1029/2001GL014144.
- Hsu, C. T., and B. Fattahi (1976), Mechanism of tornado funnel formation, *Phys. Fluids*, 19(12), 1853–1858.
- Idso, S. B. (1974), Tornado or dust devil, the enigma of desert whirlwinds, *Am. Sci.*, 62, 530–541.
- Idso, S. B. (1975), Observations of dust devils over water, *Bull. Am. Meteorol. Soc.*, 56, 376.
- Iversen, J. D., and B. White (1982), Saltation threshold on Earth, Mars and Venus, *Sedimentology*, 29, 111–119.
- Ives, R. L. (1947), Behavior of dust devils, *Bull. Am. Meteorol. Soc.*, 28, 168–174.
- Kahn, R. A., T. Z. Martin, R. W. Zurek, and S. W. Lee (1992), The Martian dust cycle, in *Mars*, edited by H. H. Kieffer et al., pp. 1017–1053, Univ. of Ariz. Press, Tucson.
- Kaimal, J. C., and J. A. Bussinger (1970), Case studies of a convective plume and a dust devil, *J. Appl. Meteorol.*, 9, 612–620.
- Kanak, K. M. (2005), Numerical simulation of dust devil-scale vortices, *Q. J. R. Meteorol. Soc.*, 131, 1271–1292.
- Kanak, K. M., D. Lilly, and J. T. Snow (2000), The formation of vertical vortices in the convective boundary layer, *Q. J. R. Meteorol. Soc.*, 126, 2789–2810.
- Lemmon, M. T., et al. (2004), Atmospheric imaging results from the Mars Exploration Rovers: Spirit and Opportunity, *Science*, 306, 1753–1756.
- Liu, J., M. I. Richardson, and R. J. Wilson (2003), An assessment of the global, seasonal, and interannual spacecraft record of Martian climate in the thermal infrared, *J. Geophys. Res.*, 108(E8), 5089, doi:10.1029/2002JE001921.
- Lorenz, R. D., and M. J. Myers (2005), Dust devil hazard to aviation: A review of United States air accident reports, *J. Meteorol.*, 30(298), 178–184.
- Magalhaes, J. A., J. T. Schofield, and A. Seiff (1999), Results of the Mars Pathfinder atmospheric structure investigation, *J. Geophys. Res.*, 104, 8943–8955.
- Malin, M. C., and K. S. Edgett (2001), Mars Global Surveyor Mars Orbiter Camera: Interplanetary cruise through primary mission, *J. Geophys. Res.*, 106, 23,429–23,570.
- Mattsson, J. O., T. Nihlén, and W. Yue (1993), Observations of dust devils in a semi-arid district of southern Tunisia, *Weather*, 48, 359–363.
- McGinnigle, J. B. (1966), Dust whirls in north-west Libya, *Weather*, 21, 272–276.
- Metzger, S. M. (1999), Dust devils as aeolian transport mechanisms in southern Nevada and in the Mars Pathfinder landing site, Ph.D. thesis, Univ. of Nev., Reno.
- Metzger, S. (2001), Recent advances in understanding dust devil processes and sediment flux on Earth and Mars, *Lunar Planet. Sci.* [CD-ROM], XXXII, Abstract 2157.
- Metzger, S. (2005), Evidence of dust devil scour at the MER Spirit Gusev site, *Lunar Planet. Sci.* [CD-ROM], XXXVI, Abstract 2397.
- Metzger, S. M., and N. Lancaster (1995), Dust devil activity in a playa basin, southern Nevada, *Eos Trans. AGU*, 76(46), Fall Meet. Suppl., F66.
- Metzger, S. M., J. R. Carr, J. R. Johnson, T. J. Parker, and M. T. Lemmon (1999), Dust devil vortices seen by the Mars Pathfinder camera, *Geophys. Res. Lett.*, 26, 2781–2784.
- Metzger, S. M., J. R. Carr, J. R. Johnson, T. J. Parker, and M. T. Lemmon (2000), Techniques for identifying dust devils in Mars Pathfinder images, *IEEE Trans. Geosci. Remote Sens.*, 38(2), 870–876.
- Metzger, S., M. R. Balme, W. M. Farrell, S. Fuerstenau, R. Greeley, J. Merrison, M. R. Patel, T. J. Ringrose, M. C. Towner, and J. C. Zarnecki (2004a), Unwrapping the whirlwind: Measuring natural dust devils, *Geol. Soc. Am. Abstr. Programs*, 36(5–11), 22.
- Metzger, S., M. R. Balme, R. Greeley, T. J. Ringrose, M. C. Towner, and J. C. Zarnecki (2004b), Surface profiling of natural dust devils, *Lunar Planet. Sci.* [CD-ROM], XXXV, Abstract 2063.
- Michaels, T. I., and S. C. R. Rafkin (2001), Simulation of the convective boundary layer and dust devils on Mars, paper presented at 33rd Annual Meeting, Div. for Planet. Sci. of the Am. Astron. Soc., New Orleans, La.
- Morton, B. R. (1966), Geophysical vortices, *Prog. Aeronaut. Sci.*, 7, 145–194.
- Murphy, J., and S. Nelli (2002), Mars Pathfinder convective vortices: Frequency of occurrence, *Geophys. Res. Lett.*, 29(23), 2103, doi:10.1029/2002GL015214.
- Neakrase, L. D. V., R. Greeley, and J. D. Iversen (2004), Dust devils on Mars: Scaling of dust flux based on laboratory simulations, *Lunar Planet. Sci.* [CD-ROM], XXXV, Abstract 1395.
- Neubauer, F. M. (1966), Thermal convection in the Martian atmosphere, *J. Geophys. Res.*, 71, 2419–2426.
- Newman, C. E., S. R. Lewis, P. L. Read, and F. Forget (2002), Modeling the Martian dust cycle: 1. Representations of dust transport processes, *J. Geophys. Res.*, 107(E12), 5123, doi:10.1029/2002JE001910.
- Pollack, J. B., D. S. Colburn, F. M. Flasar, R. Kahn, C. E. Carlston, and D. Pidek (1979), Properties and effects of dust particles suspended in the Martian atmosphere, *J. Geophys. Res.*, 84, 2929–2945.
- Pollack, J. B., M. E. Ockert-Bell, and M. K. Shepard (1995), Viking Lander image analysis of Martian atmospheric dust, *J. Geophys. Res.*, 100, 5235–5250.
- Rafkin, S., B. Haberle, and T. Michaels (2001), The Mars regional atmospheric modelling system: Model description and selected simulations, *Icarus*, 151, 228–256.
- Renno, N. O., and H. B. Bluestein (2001), A simple theory for waterspouts, *J. Atmos. Sci.*, 58, 927–932.
- Renno, N. O., and A. P. Ingersoll (1996), Natural convection as a heat engine: A theory for CAPE, *J. Atmos. Sci.*, 53, 572–585.
- Renno, N. O., M. L. Burkett, and M. P. Larkin (1998), A simple thermodynamical theory for dust devils, *J. Atmos. Sci.*, 55, 3244–3252.
- Renno, N. O., A. A. Nash, J. Lunine, and J. Murphy (2000), Martian and terrestrial dust devils: Test of a scaling theory using Pathfinder data, *J. Geophys. Res.*, 105, 1859–1865.
- Renno, N. O., et al. (2004), MATADOR 2002: A pilot field experiment on convective plumes and dust devils, *J. Geophys. Res.*, 109, E07001, doi:10.1029/2003JE002219.
- Richardson, M. I. (1998), Comparison of microwave and infrared measurements of Martian atmospheric temperatures: Implications for short-term climate variability, *J. Geophys. Res.*, 103, 5911–5918.
- Ringrose, T. J. (2003), An investigation of Martian and terrestrial dust devils, Ph.D. thesis, The Open Univ., Milton Keynes, U.K.

- Ringrose, T. J., M. C. Towner, and J. C. Zarnecki (2003), Convective vortices on Mars: A reanalysis of Viking Lander 2 meteorological data, sols 1–60, *Icarus*, *163*, 78–87.
- Rossi, A. P. (2002), Possible dust devils tracks detected in Tenere Desert, (Niger): An analogue to Mars, *Lunar Planet. Sci.* [CD-ROM], *XXXIII*, Abstract 1307.
- Rover Team (1997), Characterization of the Martian surface deposits by the Mars Pathfinder rover, Sojourner, *Science*, *278*, 1765–1767.
- Ruff, S. W., and P. R. Christensen (2002), Bright and dark regions on Mars: Particle size and mineralogical characteristics based on Thermal Emission Spectrometer data, *J. Geophys. Res.*, *107*(E12), 5127, doi:10.1029/2001JE001580.
- Ryan, J. A. (1972), Relation of dust devil frequency and diameter to atmospheric temperature, *J. Geophys. Res.*, *77*, 7133–7137.
- Ryan, J. A., and J. J. Carroll (1970), Dust devil wind velocities: Mature state, *J. Geophys. Res.*, *75*, 531–541.
- Ryan, J. A., and R. D. Lucich (1983), Possible dust devils, vortices on Mars, *J. Geophys. Res.*, *88*, 11,005–11,011.
- Schofield, J. T., J. R. Barnes, D. Crisp, R. M. Haberle, S. Larsen, J. A. Magalhaes, J. R. Murphy, A. Seiff, and G. Wilson (1997), The Mars Pathfinder atmospheric structure investigation meteorology (ASIMET) experiment, *Science*, *278*, 1752–1758.
- Schwiesow, R. L., and R. E. Cupp (1975), Remote Doppler velocity measurements of atmospheric dust devil vortices, *Appl. Opt.*, *15*, 1–2.
- Schwiesow, R. L., R. E. Cupp, M. J. Post, P. C. Sinclair, and R. F. Abbey (1977), Velocity structures of waterspouts and dust devils as revealed by Doppler lidar measurements, *Bull. Am. Meteorol. Soc.*, *58*, 677.
- Sinclair, P. C. (1964), Some preliminary dust devil measurements, *Mon. Weather Rev.*, *22*(8), 363–367.
- Sinclair, P. C. (1965), On the rotation of dust devils, *Bull. Am. Meteorol. Soc.*, *46*, 388–391.
- Sinclair, P. C. (1966), General characteristics of dust devils, Ph.D. thesis, Univ. of Ariz., Tucson.
- Sinclair, P. C. (1969), General characteristics of dust devils, *J. Appl. Meteorol.*, *8*, 32–45.
- Sinclair, P. C. (1973), The lower structure of dust devils, *J. Atmos. Sci.*, *30*, 1599–1619.
- Smith, M. D. (2004), Interannual variability in TES atmospheric observations of Mars during 1999–2003, *Icarus*, *167*, 148–165.
- Smith, P. H., and M. T. Lemmon (1999), Opacity of the Martian atmosphere measured by the imager for Mars Pathfinder, *J. Geophys. Res.*, *104*, 8975–8985.
- Smith, P. H., and Mars Pathfinder Team (1997), Results from the Mars Pathfinder camera, *Science*, *278*, 1758–1765.
- Snow, J. T., and T. M. McClelland (1990), Dust devils at White Sands Missile Range, New Mexico: 1. Temporal and spatial distributions, *J. Geophys. Res.*, *95*, 13,707–13,721.
- Stanzel, C., M. Pätzold, A. Wennmacher, E. Hauber, G. Neukum, and the HRSC CoI Team (2005), First estimates of the forward velocity of Martian dust devils from HRSC images, *Geophys. Res. Abstr.*, *7*, Abstract 06497.
- Thomas, P. C., and P. J. Gierasch (1985), Dust devils on Mars, *Science*, *230*, 175–177.
- Toigo, A. D., and M. I. Richardson (2002), A mesoscale model for the Martian atmosphere, *J. Geophys. Res.*, *107*(E7), 5049, doi:10.1029/2000JE001489.
- Toigo, A. D., M. I. Richardson, S. P. Ewald, and P. J. Gierasch (2003), Numerical simulation of Martian dust devils, *J. Geophys. Res.*, *108*(E6), 5047, doi:10.1029/2002JE002002.
- Tomasko, M. G., L. R. Doose, M. Lemmon, P. H. Smith, and E. Wegryn (1999), Properties of dust in the Martian atmosphere from the Imager on Mars Pathfinder, *J. Geophys. Res.*, *104*, 8987–9007.
- Towner, M. C., T. J. Ringrose, M. R. Patel, M. R. Balme, S. Metzger, R. Greeley, and J. C. Zarnecki (2004), A close encounter with a terrestrial dust devil, *Lunar Planet. Sci.* [CD-ROM], *XXXV*, Abstract 1259.
- Tratt, D. M., M. H. Hecht, D. C. Catling, E. C. Samulon, and P. H. Smith (2003), In situ measurements of dust devil dynamics: Toward a strategy for Mars, *J. Geophys. Res.*, *108*(E11), 5116, doi:10.1029/2003JE002161.
- Wennmacher, A., F. M. Neubauer, M. Pätzold, and K. Schmitt (1996), A search for dust devils on Mars, *Lunar Planet. Sci.*, *XXVII*, Abstract 1417.
- Williams, N. R. (1948), Development of dust whirls and similar small-scale vortices, *Bull. Am. Meteorol. Soc.*, *29*, 106–117.
- Young, L. D. G. (1971), Interpretation of high-resolution spectra of Mars. II. Calculations of CO₂ abundance, rotational temperature, and surface pressure, *J. Quant. Spectros. Radiat. Transfer*, *11*, 1075–1086.
- Zurek, R. W., J. R. Barnes, R. M. Haberle, J. B. Pollack, J. E. Tillman, and C. B. Leovy (1992), Dynamics of the atmosphere of Mars, in *Mars*, edited by H. H. Kieffer et al., pp. 835–933, Univ. of Ariz. Press, Tucson.

M. Balme, Department of Earth Sciences, Open University, Walton Gate, Milton Keynes MK7 6AA, UK. (mattbalme@yahoo.com)

R. Greeley, Department of Geological Sciences, Arizona State University, Box 871404, Tempe, AZ 85287, USA. (greeley@asu.edu)